Received: 22 October 2019 | Revised: 30 June 2021 | Accepted: 1 July 2021

DOI: 10.1002/rnc.5712

SPECIAL ISSUE ARTICLE

Robust adaptive model predictive control for guaranteed fast and accurate stabilization in the presence of model errors†

Karime Pereida* | Lukas Brunke | Angela P. Schoellig

Institute for Aerospace Studies, University of Toronto, Ontario, Canada

Correspondence
*Corresponding author Karime Pereida, Institute for Aerospace Studies, University of Toronto, Toronto, ON, M3H 5T6, Canada.
Email: karime.pereida@robotics.utias.utoronto.ca

Summary

Numerous control applications, including robotic systems such as unmanned aerial vehicles or assistive robots, are expected to guarantee high performance despite being deployed in unknown and dynamic environments where they are subject to disturbances, unmodeled dynamics, and parametric uncertainties. The fast feedback of adaptive controllers makes them an effective approach for compensating for disturbances and unmodeled dynamics, but adaptive controllers seldom achieve high performance, nor do they guarantee state and input constraint satisfaction. In this paper we propose a robust adaptive model predictive controller for guaranteed fast and accurate stabilization in the presence of model uncertainties. The proposed approach combines robust model predictive control (RMPC) with an underlying discrete-time $\mathscr{L}_1$ adaptive controller. We refer to this combined controller as an RMPC-$\mathscr{L}_1$ controller. The $\mathscr{L}_1$ adaptive controller forces the system to behave close to a linear reference model despite the presence of parametric uncertainties. However, the true dynamics of the $\mathscr{L}_1$ adaptive controlled system may deviate from the linear reference model. In this work we prove that this deviation is bounded and use it as the modeling error of the linear reference model. We combine $\mathscr{L}_1$ adaptive control with an RMPC that leverages the linear reference model and the modeling error. We prove stability and recursive feasibility of the proposed RMPC-$\mathscr{L}_1$. Further, we validate the feasibility, performance, and accuracy of the proposed RMPC-$\mathscr{L}_1$ on a stabilization task in a numerical experiment. We demonstrate that the proposed RMPC-$\mathscr{L}_1$ outperforms $\mathscr{L}_1$ adaptive control, robust MPC, and other baseline controllers in all metrics.

KEYWORDS:
robust adaptive control, model predictive control, model uncertainty

1 | INTRODUCTION

Unknown or changing operational environments — such as those found in autonomous driving, assistive robotics, and unmanned aerial vehicles applications — are difficult to model. As a result, unknown disturbances, changing dynamics, and parametric uncertainties may significantly deteriorate the performance and cause instability of traditional, model-based controllers (see[1] and[2]). To be robust to unknown disturbances, controllers must be quick to adapt to changing conditions. In regimes for which accurate models are difficult to obtain, fast controller update rates are therefore indispensable for achieving high performance.

†Final published article at the *International Journal of Robust and Nonlinear Control*: https://doi.org/10.1002/rnc.5712

In this work we propose to combine an underlying ℓ_1 adaptive controller (ℓ_1 AC) with a *robust* model predictive controller (RMPC). The resulting robust adaptive model predictive controller, RMPC-ℓ_1, achieves high performance and accurate stabilization in the presence of model errors. The ℓ_1 adaptive controller forces a system to behave close to a specified linear reference model despite the presence of parametric uncertainties. We show that the ℓ_1 controlled system may deviate from the specified linear reference model, but this deviation, which can be used as a modeling error, is bounded. The RMPC computes a reference for the underlying adaptive controller while explicitly taking into account the bound on the modeling error, the linear reference model, and state and input constraints. The RMPC improves the performance and aggressiveness of the underlying ℓ_1 controlled system. Additionally, the underlying ℓ_1 AC consistently reduces the modeling error at every time step and enables accurate stabilization to the origin. Explicitly taking into account the modeling error from the underlying ℓ_1 AC enables the proposed robust adaptive MPC to guarantee feasibility for more initial conditions than using ℓ_1 AC or RMPC separately. Note that in this work we use $\mathcal{L}_1$ to refer to the continuous-time formulation, and ℓ_1 to refer to the discrete-time adaptive control formulation.

1.1 | Related Work

$\mathcal{L}_1$ adaptive control generates a control signal that forces a system to track a reference trajectory according to a specified linear reference model despite the presence of parametric uncertainties or unknown disturbances. The architecture of the $\mathcal{L}_1$ adaptive controller decouples the estimation loop from the control law. Consequently, there is guaranteed robustness in the presence of fast adaptation, without introducing persistence of excitation, gain scheduling in the controller parameters, or high-gain feedback[3]. $\mathcal{L}_1$ adaptive control has been extensively developed for continuous-time applications[3,4,5] and has been applied to different platforms such as an underwater vehicle[6], a tailless fighter aircraft in simulation[7], bipedal robots in simulation[8], and a quadrotor, hexacopter, and octocopter[9]. However, $\mathcal{L}_1$ adaptive control has not been developed as extensively for discrete-time applications[10,11].

Model predictive control (MPC) has been widely employed to control constrained systems, and an extensive literature on the subject exists[12,13,14]. MPC solves a finite-horizon optimal control problem at each time step to calculate a control sequence that minimizes a given objective function according to a system model and constraints. A controller is said to be robust when stability is maintained and performance specifications are met for a specified range of model variations and a class of noise signals[15]. The standard implementation of MPC, using a nominal model of the system dynamics, exhibits nominal robustness to small disturbances under certain assumptions. The main assumption is that no hard state constraints are considered (see details in chapter 3.2 in[16]). This may be insufficient if the conditions are not met and larger disturbances are present[13,17]. The term *nominal* MPC is used in this work to describe the standard implementation of MPC[12]. In order to achieve robustness to larger disturbances, numerous MPC methods have been considered. The simplest is to ignore the disturbances and rely on the inherent robustness of deterministic MPC applied to the nominal system[16]. In these approaches the so-called spread of predicted trajectories resulting from disturbances is not acknowledged.

Various open- and closed-loop MPC methods have been developed that acknowledge such disturbances. *Open-loop* methods calculate the control action that is safe enough to cope with the effect of the worst disturbance realization[18]. These controllers can be very conservative as the disturbance effect can be mitigated by feedback in the actual operation. For this reason, *closed-loop* prediction is introduced in[19]. The work in[20] proposed a feedback MPC where the decision variable is a policy consisting in a sequence of control laws. Nevertheless, determining a control policy can be prohibitively difficult, and simplifying approximations have been proposed[21,22,23]. A popular branch of robust MPC is based on the idea of tubes, as presented in[22] for linear systems. In[24] a robust MPC for nonlinear systems based on tubes was proposed and achieved good tracking performance in simulation. However, determining the tightened state and input constraints and the added computational cost of solving a nonlinear optimization problem remains a challenge. A survey on robust MPC can be found in[25].

One way to handle model uncertainties is to develop robust MPC methods, as described above. Another way to handle model uncertainties is through adaptive MPC. In[26] an adaptive MPC for a class of constrained linear systems, that estimates parameters online is presented. However, parameter adaptation depends on state excitation. The performance of the proposed approach is shown in simulation. The work in[27] proposed an adaptive MPC for linear systems with parametric uncertainties. At each timestep, the adaptation law updates the estimated model parameters and uses the updated model to solve an MPC problem. However, additional constraints must be added to the MPC problem in order to guarantee an estimation error bound. These results are shown in a simulation example. It is difficult to guarantee the fulfillment of constraints in the presence of an adaptive mechanism. Further, it is difficult to guarantee feasibility and stability theoretically when an adaptation is introduced to MPC[26].

Robust adaptive control helps adaptive controllers achieve robustness. A number of robust adaptive MPC schemes have been proposed. The work by[28] proposes a robust adaptive MPC for time-invariant and time-varying uncertain finite impulse response (FIR) models. In this linear MPC approach, the uncertainty of the model is assumed to be in a given parameter set. At each timestep *(i)* a recursive set-membership identification algorithm tracks the set of all possible model parameters that are consistent with the initial assumptions and the data collected thus far, and *(ii)* a robust MPC minimizes the cost function while guaranteeing satisfaction of constraints for all parameters in the feasible parameter set. In order to reduce computational complexity (which could grow linearly with time), further assumptions have to be made, e.g. that the parameters lie in a larger set. The latter could incur in a conservative controller. This approach is restricted to stable systems, because it relies on FIR models. The work in[29] extends the work in[28] to a state space formulation, which removes the restriction to stable systems. The extended approach consists of a robust MPC with recursive model update for linear systems with time invariant parametric uncertainty and additive disturbance. Set-membership estimation combined with a homothetic tube is proposed. Additionally, the approach in[29] uses polytopic uncertainty sets resulting in poor scalability of the adaptation of the uncertainty with system dimension. An adaptive stochastic MPC for linear state-space systems under time-varying uncertainty is presented in[30]. The linear model is assumed to accurately model the system, which has a bounded additive uncertainty with a bounded rate of change. The parametric uncertainty lies in the feasible parameter set, which is updated at every time step with a set-membership method (the adaptive component of this framework). The feasible parameter set is used by a stochastic MPC to compute an input that is feasible for all the possible uncertainties in the adapted feasible parameter set. Simulation results show that the proposed approach satisfies constraints robustly (admissible probability of constraint violation is 0) or stochastically. Robust adaptive MPC approaches have also been proposed for nonlinear systems. A robust adaptive MPC is proposed in [31] for linearly parameterized uncertain nonlinear systems subject to state and input constraints. Here, the set-based estimation is updated only when non-expansion of the set is guaranteed, reducing the conservativeness of this approach. No claims are made regarding the computational requirements of this approach, however.

Control architectures that combine an outer MPC and an inner controller that forces the system to match an *a priori* specified closed-loop model have been proposed. In[32] a data-driven control for constrained systems is proposed. An inner data-driven linear time-invariant or linear parameter-varying controller is designed to match an *a priori* specified closed-loop model. The inner controller requires previously recorded data of the system input, output, and exogenous signal to be tuned offline. Further, an outer MPC is designed to handle input and output constraints and to enhance the performance of the inner loop. In[33], an inner data-driven controller uses system data to parameterize a linear controller for which the closed-loop system matches a given strictly-proper reference model. The inner controller can be implemented such that the control parameters are tuned online. Moreover, an outer loop MPC acts as a reference governor, which selects the optimal reference to be supplied to the inner controller to improve the performance of the system. Related non-MPC methods for stabilization or reference tracking under uncertainty use contraction methods combined with $\mathcal{L}_1$ adaptive control[34]. However, these methods do not leverage prediction models, which can yield conservative behavior.

In previous work[35] we proposed an adaptive MPC that combines an underlying $\mathcal{L}_1$ adaptive controller with a nominal MPC. In this way, adaptation is decoupled from the optimization problem. The $\mathcal{L}_1$ adaptive controller forces a system to behave close to a specified linear reference model despite the presence of parametric uncertainties and unknown disturbances. The nominal MPC uses this linear reference model to improve the trajectory tracking performance of the $\mathcal{L}_1$ controlled system. This architecture achieves high tracking performance of a possibly nonlinear system at the computational cost of a linear MPC even when disturbances are applied. Experiments on a drone showed that the adaptive MPC approach is able to achieve high accuracy trajectory tracking even when wind disturbances are applied to the vehicle. However, this approach assumes that the linear model exactly represents the underlying adaptive system, which may degrade the performance of the controller when modeling errors are present.

1.2 | Our Contributions

In order to deal with model uncertainties and further improve performance, we propose RMPC-ℓ_1, a robust and adaptive MPC. The main contributions of this work are: *(i)* introducing a modified discrete-time state feedback ℓ_1 adaptive controller; *(ii)* providing stability and performance proofs for the proposed approach; and *(iii)* validating the feasibility, performance, and accuracy of the proposed RMPC-ℓ_1 on a stabilization task. The proposed robust adaptive MPC decouples adaptation from robustness with two main components: *(i)* an underlying discrete-time state feedback ℓ_1 adaptive controller (orange dashed box in Fig. 1); and *(ii)* a robust MPC (blue box in Fig. 1). The ℓ_1 adaptive controller makes the system behave close to a linear reference model

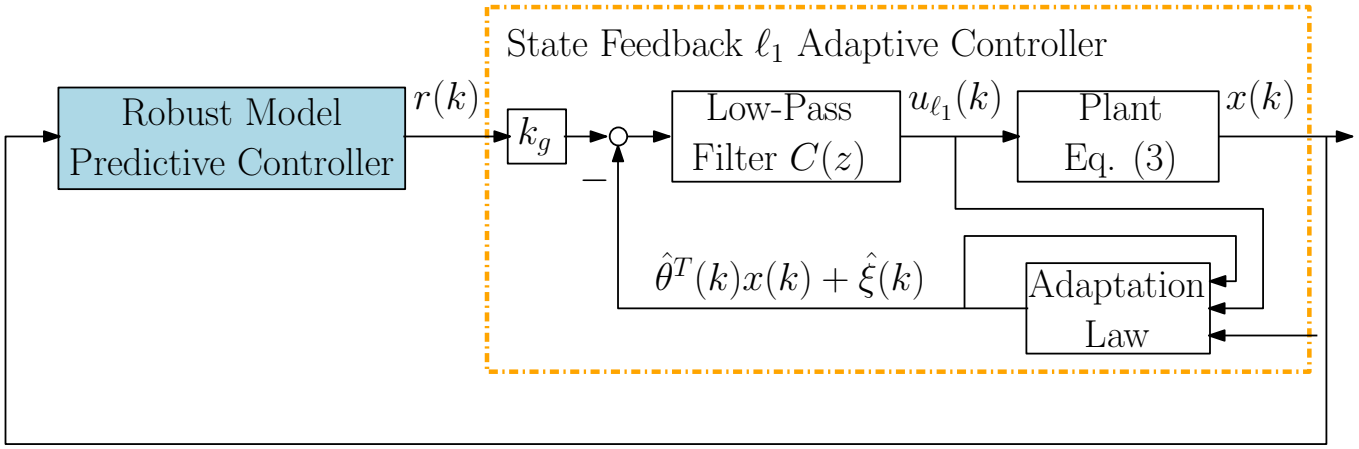

FIGURE 1 Proposed RMPC-$\mathscr{\ell}_1$ framework to achieve high-performance control in the presence of modeling errors. The discrete-time state feedback $\mathscr{\ell}_1$ adaptive controller makes the system behave close to a specified reference linear system despite parametric uncertainties. The difference between the state of the reference system and the state of the $\mathscr{\ell}_1$ controlled system is bounded and can be considered as a modeling error. The robust model predictive controller improves the performance at each time step, using the specified reference system as well as the modeling error.

despite parametric uncertainties, for which we specify upper bounds. The $\mathscr{\ell}_1$ controlled system state may deviate from the linear reference model state, which results in a modeling error. In this work, we show that this deviation is upper bounded and realizable. The upper bound and the linear reference model are used in an RMPC framework to calculate the input that minimizes a user-specified cost function for the $\mathscr{\ell}_1$ controlled system. Intuitively, the modeling error –characterized by the upper bound on the difference between the linear reference model and the $\mathscr{\ell}_1$ controlled system– can be viewed as an additive disturbance affecting the linear reference model. Note that robust MPC frameworks such as the ones presented by[22] and[23] are proposed for linear systems with bounded additive disturbances; hence, they can be used in our framework.

The proposed robust adaptive MPC requires the following changes with respect to[35]: *(i)* the $\mathscr{\ell}_1$ adaptive controller is state feedback instead of output feedback, and *(ii)* the $\mathscr{\ell}_1$ adaptive controller is formulated in discrete time. These two changes enable the computation of a bound on the modeling error, which is required by the robust MPC. The first change is motivated because a state feedback $\mathscr{\ell}_1$ adaptive controller attains performance bounds that are realizable. The output feedback $\mathscr{L}_1$ adaptive controller used in[35] describes the system with a transfer function $A(s)$, which is a strictly-proper but *unknown*. This transfer function is present in all the performance bounds, which makes them difficult to calculate. Unlike output feedback, state feedback $\mathscr{\ell}_1$ adaptive controllers decouple the system uncertainties from the performance bounds. Hence, it is possible to calculate these bounds. The $\mathscr{\ell}_1$ adaptive controller in this work is designed in the discrete time to improve robustness in the implementation. Typically, a discretized version of the continuous time $\mathscr{L}_1$ adaptive control is implemented[4,36,35,37]. However, if the sampling time is increased, the discretized version can become unstable, as shown in[38]. The second change is motivated since MPC frameworks are generally formulated for discrete-time systems. Moreover, we derive the uniform bound of the difference between the state of the linear reference model and the state of the $\mathscr{\ell}_1$ controlled system, and leverage it in the robust MPC. In a numerical experiment we show that the proposed RMPC-$\mathscr{\ell}_1$ outperforms $\mathscr{\ell}_1$ AC and RMPC on a stabilization task when they are used separately according to three metrics. First, the proposed RMPC-$\mathscr{\ell}_1$ increases the number of feasible initial conditions compared to baseline controllers that include $\mathscr{\ell}_1$ adaptive controller and RMPC used individually. Second, RMPC-$\mathscr{\ell}_1$ achieves a similar or better performance than RMPC when both approaches use the same user-specified cost function. Finally, the proposed RMPC-$\mathscr{\ell}_1$ controls the system from any state in its robust controllable set to the origin accurately and in a limited number of time steps. Both $\mathscr{\ell}_1$ AC and RMPC fail to accurately bring the state to the origin in a finite number of time steps, because they are either less aggressive or are not able to reduce the modeling error. The robust adaptive MPC proposed in this paper does not have the computational cost of approaches that have set membership estimation[28,30,29,31]. Moreover, the concept and implementation are simple since it combines a standard robust MPC with an $\mathscr{\ell}_1$ adaptive controller. Contrary to works that require a FIR model (e.g.,[28]), the system in our work need not be stable, only controllable. A limitation of our work is that it does not take into account time-varying uncertainties and disturbances; however, our proposed approach could be extended to these cases with an appropriately designed

underlying $\mathscr{L}_1$ adaptive controller. Unlike[32,33], our proposed RMPC-$\mathscr{L}_1$ approach is able to bound the modeling errors in the underlying controller and later account for them in the RMPC framework. Preliminary results of this work were presented in[39].

2 | PROBLEM FORMULATION

The objective of this work is to achieve fast and accurate stabilization in the presence of modeling errors, while guaranteeing feasibility for as many initial conditions as possible. Consider the class of discrete-time systems with matched constant uncertainties θ, ξ whose dynamics can be described by the following system:

$$\begin{aligned} x(k+1) &= Ax(k) + b_m(u(k) + \theta^T x(k) + \xi)\,,\ x(0) = x_0\,, \\ y(k) &= c_m^T x(k)\,, \end{aligned} \tag{1}$$

where $x(k) \in \mathbb{X} \subset \mathbb{R}^n$ is the system state vector (assumed to be measured); $u(k) \in \mathbb{U} \subset \mathbb{R}$ is the control signal; b_m, $c_m \in \mathbb{R}^n$ are known constant vectors; A is the known $n \times n$ matrix, with $(A\,, b_m)$ controllable; θ is a vector of *unknown* parameters, and ξ is an unknown parameter belonging to the compact convex sets $\theta \in \Theta \subset \mathbb{R}^n$ and $\xi \in \Xi \subset \mathbb{R}$, respectively; and $y(k) \in \mathbb{R}$ is the regulated output.

Assumption 1. The set Θ is compact and convex. Each dimension i is bounded by $L_{\Theta_{i,\min}} \leq \theta_i \leq L_{\Theta_{i,\max}}$ and the set Θ includes all the values that satisfy this criterion.

The parameter ξ is bounded by $L_{\xi,\min} \leq \xi \leq L_{\xi,\max}$ where Ξ is the set that includes all the values that satisfy this criterion.

Generally, the unknown parameters model physical attributes of the system such as mass, moment of inertia, friction, among others. For this reason we assume these parameters lie in a compact, convex set.

The goal is to stabilize the system to the origin in a finite number of steps $N < \infty$ while minimizing a given quadratic objective function for high-performance control, without violating any state or input constraints $\mathbb{X}$ and $\mathbb{U}$, despite the presence of parametric uncertainties in the system. The resulting controller must be stable and provide high performance for a variety of initial conditions.

3 | DISCRETE-TIME STATE FEEDBACK $\mathscr{L}_1$ ADAPTIVE CONTROL

In this section we present a modified discrete-time $\mathscr{L}_1$ adaptive controller along with proofs for stability and performance guarantees. Recall that the $\mathscr{L}_1$ adaptive controller brings two important features for the overall robust adaptive MPC. First, it forces the controlled system to behave close to a linear reference model despite the presence of unknown parameters. Second, it provides an upper bound for the modeling error that arises between the controlled system and the linear reference model. The discrete-time state feedback $\mathscr{L}_1$ adaptive controller is inspired by[10]; however, in this work we *(i)* extend the system to include an unknown parameter ξ (see (1)), *(ii)* modify the adaptation law to avoid division by zero, and *(iii)* prove the uniform upper bound on the difference between state of the $\mathscr{L}_1$ controlled system and the state of the linear reference model.

There are two main design challenges for a discrete-time state feedback $\mathscr{L}_1$ adaptive controller: *(i)* the definition of an adaptation law, and *(ii)* the mechanism to guarantee that the estimated parameters remain in a given set. The first challenge is the definition of an adaptation law that allows us to show stability and performance guarantees. The adaptation law is fundamentally a parameter estimation scheme. Parameter estimation for deterministic discrete-time systems has been widely studied[40,41]. Some of these algorithms have been used in discrete-time model reference adaptive control (MRAC) frameworks[42] and discrete-time $\mathscr{L}_1$ adaptive controllers[10]. The second challenge is guaranteeing that the estimated parameters remain in a given set. The latter facilitates the stability analysis and derivation of performance guarantees for the $\mathscr{L}_1$ adaptive controller, as will be shown in this section. To guarantee that the estimated parameters remain in a given set, the continuous-time $\mathcal{L}_1$ adaptive controllers use the projection operator[3]. To derive similar performance guarantees in discrete time, the adaptation law used for the $\mathscr{L}_1$ adaptive controller must also include a projection. Given these design challenges, the adaptation law in this work is based on the orthogonalized projection algorithm described in[41].

Considering the class of systems described in (1), the control objective of the $\mathscr{L}_1$ adaptive controller is to design an adaptive state feedback control signal $u_{\mathscr{L}_1}(k)$ such that the system output $y(k)$ tracks the discrete-time, bounded reference signal $r(k)$ with quantifiable transient and steady-state performance bounds. The output is required to track the reference according to a specified stable reference system.

3.1 | Discrete-Time State Feedback ℓ_1 Adaptive Control Architecture

We consider the following control structure:

$$u(k) = u_m(k) + u_{\ell_1}(k), \quad u_m(k) = -k_m^T x(k), \tag{2}$$

where $k_m \in \mathbb{R}^n$ renders $A_m \triangleq A - bk_m^T$ stable, while $u_{\ell_1}(k)$ is the adaptive component, which will be defined shortly. The static feedback gain k_m leads to the following partially closed-loop system:

$$\begin{aligned} x(k+1) &= A_m x(k) + b_m(u_{\ell_1}(k) + \theta^T x(k) + \xi), \; x(0) = x_0, \\ y(k) &= c_m^T x(k). \end{aligned} \tag{3}$$

Our discrete-time state feedback ℓ_1 adaptive controller designs a control signal such that the output $y(k)$ tracks a discrete-time reference signal $r(k)$ according to a specified stable reference system $A_m(k)$. The discrete-time state feedback ℓ_1 adaptive controller proposed in this work for the partially closed-loop system (3) is shown in an orange dashed box in Fig. 1. The individual components of the ℓ_1 adaptive control architecture are introduced below. This architecture is inspired by the architecture presented by [10]. The equations that describe the implementation of the discrete-time state feedback ℓ_1 adaptive controller are:

Adaptation Law:

We propose the following projection algorithm estimator[40,41] that avoids division by zero:

$$\hat{\rho}(k+1) = \hat{\rho}(k) + \frac{\begin{bmatrix} x(k) \\ 1 \end{bmatrix} \left[b_0^T(x(k+1) - A_m x(k) - b_m u_{\ell_1}(k)) - \hat{\rho}^T(k) \begin{bmatrix} x(k) \\ 1 \end{bmatrix} \right]}{1 + x^T(k)x(k)}, \quad \hat{\rho}(0) = \hat{\rho}_0 \in \Theta \times \Xi, \tag{4}$$

where $\hat{\rho}(k) = [\hat{\theta}^T(k), \; \hat{\xi}(k)]^T$, and $b_0 \triangleq \dfrac{b_m}{b_m^T b_m}$ is a constant vector. If $\hat{\rho}(k+1) \in \Theta \times \Xi$, then continue, else:

(i) orthogonally project $\hat{\rho}(k+1)$ on the boundary of $\Theta \times \Xi$ to yield $\hat{\rho}'(k+1) = [\hat{\theta}'^T(k+1), \; \hat{\xi}'(k+1)]^T$:

$$\hat{\theta}_i'(k+1) = \begin{cases} L_{\Theta_{i,\min}} & \text{if } \hat{\theta}_i(k+1) \le L_{\Theta_{i,\min}} \\ L_{\Theta_{i,\max}} & \text{if } \hat{\theta}_i(k+1) \ge L_{\Theta_{i,\max}} \\ \hat{\theta}_i(k+1) & \text{otherwise}, \end{cases}$$

$$\hat{\xi}'(k+1) = \begin{cases} L_{\xi,\min} & \text{if } \hat{\xi}(k+1) \le L_{\xi,\min} \\ L_{\xi,\max} & \text{if } \hat{\xi}(k+1) \ge L_{\xi,\max} \\ \hat{\xi}(k+1) & \text{otherwise}. \end{cases} \tag{5}$$

Since $\hat{\rho}'(k+1)$ is an orthogonal projection of $\hat{\rho}(k+1)$ onto $\Theta \times \Xi$ and since $\rho \in \Theta \times \Xi$, then as for the projection algorithm of[41]:

$$\|\hat{\rho}'(k+1) - \rho\|^2 \le \|\hat{\rho}(k+1) - \rho\|^2. \tag{6}$$

The additional steps in the adaptation law guarantee that the estimate $\hat{\rho}(k)$ remains in the set $\Theta \times \Xi$. The latter is needed for the Lyapunov analysis of the system. It is of particular importance to note that since the projection is orthogonal, then (6) holds. This allows us to develop the analysis only for $\tilde{\rho}(k) \triangleq \hat{\rho}(k) - \rho$, since $\tilde{\rho}'(k) \triangleq \hat{\rho}'(k) - \rho$ is smaller.

(ii) Finally, assign

$$\hat{\rho}(k+1) = \hat{\rho}'(k+1). \tag{7}$$

Control law:

The z-transform of the adaptive control signal is:

$$u_{\ell_1}(z) = -C(z)(\hat{\eta}(z) - k_g r(z)), \tag{8}$$

where $r(z)$ and $\hat{\eta}(z)$ are the z-transforms of the reference $r(k)$ and $\hat{\eta}(k) = \hat{\rho}^T(k) \begin{bmatrix} x(k) \\ 1 \end{bmatrix}$, respectively, $k_g \triangleq (c_m^T(I_n - A_m)^{-1}b_m)^{-1}$, and $C(z)$ (see Fig. 1) is a user-defined bounded-input, bounded-output (BIBO) stable, strictly-proper, discrete-time transfer function of a filter with gain $C(1) = 1$, and its state-space realization assumes zero initialization. It is important to note that, in

order to take the truncated z-transformation, we consider $\hat{\eta}(k)$ as a function of sample time k. In other words, we consider $\hat{\eta}(k)$ as a signal that changes with time instead of considering it as a nonlinear function of $x(k)$ and $\hat{\rho}(k)$.

Intuitively, the low-pass filter in the control law (8) ensures that the uncertainties being compensated for in the feedback loop are only those within the bandwidth of the control channel. The role of $\hat{\eta}(z)$ in the control law (8) is to cancel the parametric uncertainties $\theta^T x(k) + \xi$ affecting the system. Additionally, $r(z)$ specifies the reference which is multiplied by the gain k_g in order to ensure the tracking of the reference $r(z)$ by the output $y(z)$ in the steady state.

The discrete-time $\mathscr{L}_1$ adaptive controller is defined via (4) – (8) with $C(z)$ verifying the following $\mathscr{L}_1$-norm conditions:

$$\lambda_\theta \triangleq \|G(z)\|_{\mathscr{L}_1} L_\theta < 1\,, \quad \lambda_\xi \triangleq \|G(z)\|_{\mathscr{L}_1} L_\xi < \infty\,, \tag{9}$$

where

$$\begin{aligned} &G(z) \triangleq H(z)(1 - C(z))\,, \quad && H(z) \triangleq (zI_n - A_m)^{-1} b_m\,, \\ &L_\theta \triangleq \max_{\theta\in\Theta} \|\theta\|_1\,, && L_\xi \triangleq \max_{\xi\in\Xi} |\xi|\,. \end{aligned} \tag{10}$$

These conditions are required to guarantee stability of the system and follow from the application of the small-gain theorem[43]. Intuitively, these conditions mean that the controller should be designed such that closing the loop with the unknown parameters lying in the sets given in assumption 1 guarantees a stable closed-loop system. They are not restrictive since they give design guidelines for the low-pass filter $C(z)$ and the stabilizing gain k_m, given that the unknown parameters are assumed to lie in $\Theta\times\Xi$. Moreover, the following assumption is also required.

Assumption 2. There exists $\gamma_0 > 0$ such that the following inequality holds

$$\sqrt{\frac{\frac{1}{2}\left(e^{\tau\rho_{\max}} - 1\right)\left(1 + 4nc_2^2\right)}{1 - \frac{1}{2}\left(e^{\tau\rho_{\max}} - 1\right)\left(4nc_1^2\right)}} < \gamma_0\,, \tag{11}$$

where $\frac{1}{2}\left(e^{\tau\rho_{\max}} - 1\right) 4nc_1^2 < 1$, $\tau > 0$,

$$\rho_{\max} \triangleq 4 \max_{\rho\in\Theta\times\Xi} \|\rho\|^2\,, \tag{12}$$

$P = P^T > 0$ solves the algebraic Lyapunov equation

$$P = A_m^T P A_m + R + I_n\,, \tag{13}$$

for arbitraty symmetric $R = R^T > 0$, and $\lambda_{\min}(P)$ is the minimum eigenvalue of P. Moreover, we define c_1 and c_2 as:

$$c_1 = \frac{\lambda_\theta}{1-\lambda_\theta}\ c_2 = \frac{1}{1-\lambda_\theta}\left(\lambda_\xi + \|k_g H(z)C(z)\|_{\mathscr{L}_1} \|r\|_{\mathscr{L}_\infty} + \|x_{in}\|_{\mathscr{L}_\infty}\right)\,, \tag{14}$$

where

$$x_{in}(z) \triangleq (zI_n - A_m)^{-1} x_0\,, \tag{15}$$

captures the initial conditions.

Satisfaction of Assumption 2 depends mainly on achieving a small λ_θ, such that c_1 is small. This can be achieved by carefully designing the filter $C(z)$.

3.2 | Analysis of the $\mathscr{L}_1$ Adaptive Controller

In this subsection we analyze the $\mathscr{L}_1$ adaptive controller. First, we define a nominal state predictor and show that the prediction error dynamics are stable and the predicted state is bounded. The $\mathscr{L}_1$ adaptive controller makes the system track a reference system. We characterize this closed-loop reference system and show the transient and steady-state performance bounds of the $\mathscr{L}_1$ controlled system with respect to the reference system. Finally, we characterize an ideal reference model and introduce performance bounds of the $\mathscr{L}_1$ controlled system with respect to the ideal reference system. The ideal reference model can be used to described the $\mathscr{L}_1$ controlled system and the performance bound can be used as a bound on the modeling error. This subsection is divided in three parts *(i)* background theory required for subsequent proofs, *(ii)* transient and steady-state performance with respect to the reference model, and *(iii)* performance bounds with respect to an ideal linear system.

3.2.1 | Background

The following results are needed to show the transient and steady-state performance bounds. We present them next to improve readability of the main results of the paper.

We first introduce the following notation $\|(\cdot)|_k\|_{\ell_\infty}$, which represents the ℓ_∞-norm of signal $(\cdot)$ truncated at time step k. We use a state predictor and its corresponding error dynamics as tools to show stability of the prediction error dynamics and to show performance bounds of the ℓ_1 controlled system. Note that in order to keep ℓ_1 adaptive control naming convention, we use *state predictor* to refer to a nominal prediction. We consider the following state predictor:

$$\begin{aligned} &\hat{x}(k+1) = A_m\hat{x}(k) + b_m\left(u_{\ell_1}(k) + \hat{\rho}^T(k)\begin{bmatrix}x(k)\\1\end{bmatrix}\right),\ \hat{x}(0) = x_0\,,\\ &\hat{y}(k) = c_m^T\hat{x}(k)\,, \end{aligned} \tag{16}$$

where $\hat{x}(k) \in \mathbb{R}^n$ is the state predictor and $\hat{\rho}(k) \triangleq \begin{bmatrix}\hat{\theta}(k)\\ \hat{\xi}(k)\end{bmatrix} \in \mathbb{R}^{n+1}$ is the adaptive estimate of parameters θ and ξ.

Next, we derive the error dynamics of the state predictor from (3) and (16):

$$\tilde{x}(k+1) = A_m\tilde{x}(k) + b_m(\tilde{\theta}^T(k)x(k) + \tilde{\xi}(k))\,,\quad \tilde{x}(0) = 0\,, \tag{17}$$

where $\tilde{x}(k) = \hat{x}(k) - x(k)$, $\tilde{\theta}(k) \triangleq \hat{\theta}(k) - \theta$, and $\tilde{\xi}(k) \triangleq \hat{\xi}(k) - \xi$. Let $\tilde{\eta}(k) \triangleq \begin{bmatrix}\tilde{\theta}(k)\\ \tilde{\xi}(k)\end{bmatrix}^T \begin{bmatrix}x(k)\\1\end{bmatrix}$ and $\tilde{\eta}(z)$ be its z-transform. The error dynamics (17) can be written in the z-domain as:

$$\tilde{x}(z) = H(z)\tilde{\eta}(z)\,. \tag{18}$$

We need to show that the error dynamics (18) are bounded. Lemma 1 and 2 contain results needed to show boundedness of the prediction error dynamics. In Lemma 3 we show the stability of the estimation error dynamics and a bound for the estimation error. Finally, in Lemma 4 we show that the state predictor is uniformly bounded. Lemma 1 proposes a Lyapunov function for the error dynamics of a form that is convenient to show uniform boundedness.

Lemma 1. Recall that A_m is asymptotically stable. Define

$$\sigma \triangleq \sqrt{\lambda_{\max}(A_m^T P A_m)}\,, \tag{19}$$

where $\lambda_{\max}(A_m^T P A_m)$ is the maximum eigenvalue of $A_m^T P A_m$ with P defined in (13). Let $\mu > 0$ and define:

$$V_x(\tilde{x}(k)) \triangleq \ln(1 + \mu\tilde{x}^T(k)P\tilde{x}(k)) \tag{20}$$

and

$$\Delta V_x(\tilde{x}(k)) \triangleq V_x(\tilde{x}(k+1)) - V_x(\tilde{x}(k))\,. \tag{21}$$

Then

$$\Delta V_x(\tilde{x}(k)) \le \mu\frac{-\tilde{x}^T(k)R\tilde{x}(k) + (\sigma^2+1)b_m^T P b_m[x^T(k)\tilde{\theta}(k) + \tilde{\xi}(k)]^2}{1 + \mu\tilde{x}^T(k)P\tilde{x}(k)}\,,\ k \ge 0\,. \tag{22}$$

The proof of this lemma can be found in Appendix A.1. The result of the following Lemma is required to show uniform boundedness of the error dynamics $\tilde{x}$.

Lemma 2. Assume that $\|\tilde{x}|_k\|_{\ell_\infty} \le \gamma_0$ for $k \in \{0, \dots, k'-1\}$ for a given k', where γ_0 is defined in (11). There exist constants α, $\mu > 0$ such that $\forall k \in \{0, \dots, k'-1\}$

$$1 + x^T(k)x(k) \le (1+\alpha)(1 + \mu\tilde{x}^T(k)P\tilde{x}(k))\,. \tag{23}$$

The proof of Lemma 2 can be found in Appendix A.2. Using the results presented in Lemmas 1–2, we show that the prediction error $\tilde{x}$ is uniformly bounded.

Lemma 3. The prediction error in (17) is uniformly bounded by:

$$\|\tilde{x}\|_{\ell_\infty} \le \gamma_0\,. \tag{24}$$

The proof of Lemma 3 can be found in Appendix A.3. So far we have shown that $\tilde{x}(k)$ remains bounded, but $x(k)$ and $\hat{x}(k)$ could diverge at the same rate[3]. In the next Lemma, we show that $\hat{x}(k)$ in (16), with $u_{\ell_1}(k)$ given by (8), is uniformly bounded.

Lemma 4. The state predictor in (16) is uniformly bounded by:

$$\|\hat{x}\|_{\ell_\infty} \leq \frac{\lambda_\theta \gamma_0 + \|G(z)\|_{\ell_1} L_\xi + \|H(z) k_g C(z)\|_{\ell_1} \|r\|_{\ell_\infty} + \|x_{in}\|_{\ell_\infty}}{1 - \lambda_\theta} . \tag{25}$$

The proof of this Lemma is found in Appendix A.4.

Finally, we define the following proper and BIBO stable transfer function

$$H_1(z) \triangleq C(z) \frac{1}{c_0^T H(z)} c_0^T , \tag{26}$$

where $c_0 \in \mathbb{R}^n$ and ensures that $c_0^T H(z)$ is a minimum phase transfer function with relative degree one. The full derivation is found in Appendix A.5.

3.2.2 | Transient and Steady-State Performance

The ℓ_1 adaptive controller is tracking the state of a closed-loop reference system. In this section we first characterize the closed-loop reference system for the class of systems in (3) and show that it is stable. Then, we show that the ℓ_1 controlled system tracks the closed-loop reference system in transient and steady state with quantifiable bounds. Consider the following nonadaptive version of the control system in (3) and (8) which defines the *closed-loop reference system* for the class of systems in (3):

$$\begin{aligned} x_{ref}(k+1) &= A_m x_{ref}(k) + b_m (u_{ref}(k) + \theta^T x_{ref}(k) + \xi) , \quad x_{ref}(0) = x_0 , \\ u_{ref}(z) &= -C(z)(\theta^T x_{ref}(z) + \xi - k_g r(z)) , \\ y_{ref}(k) &= c_m^T x_{ref}(k) . \end{aligned} \tag{27}$$

In the next Lemma we first show that the closed-loop reference system (27) is stable.

Lemma 5. If $\|G(z)\|_{\ell_1} L_\theta < 1$, and $\|G(z)\|_{\ell_1} L_\xi < \infty$, then (27) is bounded-input, bounded-state (BIBS) stable with respect to $r(z)$ and x_0.

Proof. From the definition in (27), it follows that:

$$x_{ref}(z) = H(z) k_g C(z) r(z) + G(z) \theta^T x_{ref}(z) + G(z) \xi + x_{in}(z) , \tag{28}$$

where $x_{in}(z)$ is defined in (15). Since $H(z)$, $C(z)$ and $G(z)$ are proper BIBO stable discrete-time transfer functions, it follows from (27) that for all $i \in \mathbb{N} \cup \{0\}$ the following bound holds:

$$\|x_{ref}|_i\|_{\ell_\infty} \leq \|H(z) k_g C(z)\|_{\ell_1} \|r|_i\|_{\ell_\infty} + \|G(z)\theta^T\|_{\ell_1} \|x_{ref}|_i\|_{\ell_\infty} + \|G(z)\xi\|_{\ell_1} + \|x_{in}|_i\|_{\ell_\infty} . \tag{29}$$

Since A_m is stable, $x_{in}(k)$ is uniformly bounded. Then, we have the following relationship

$$\|G(z)\theta^T\|_{\ell_1} = \max_{m=1,\dots,n} \|G_m(z)\|_{\ell_1} \sum_{p=1}^{n} |\theta_p| \leq \|G(z)\|_{\ell_1} L_\theta < 1 , \tag{30}$$

where $\|G_m(z)\|_{\ell_1}$ is the ℓ_1-norm for the impulse response for each output $g_m(k)$ where $m = 1, \dots, n$. Recall from Assumption 1 that $\xi \in \Xi$. Then we have the following relationship

$$\|G(z)\xi\|_{\ell_1} = \max_{m=1,\dots,n} \|G_m(z)\|_{\ell_1} |\xi| \leq \|G(z)\|_{\ell_1} L_\xi < \infty . \tag{31}$$

Consequently, we can write

$$\|x_{ref}|_i\|_{\ell_\infty} \leq \frac{\|H(z) k_g C(z)\|_{\ell_1} \|r|_i\|_{\ell_\infty} + \|G(z)\|_{\ell_1} L_\xi + \|x_{in}|_i\|_{\ell_\infty}}{1 - \|G(z)\|_{\ell_1} L_\theta} . \tag{32}$$

Since $r(k)$ and $x_{in}(k)$ are uniformly bounded, $\|G(z)\|_{\ell_1} L_\xi$ is bounded, and (32) holds uniformly for all $i \in \mathbb{N} \cup \{0\}$, $x_{ref}(k)$ is uniformly bounded. Boundedness of $y_{ref}(k)$ follows from its definition. □

We have characterized and shown that the closed-loop reference system is stable. Next, we show that the ℓ_1 controlled system tracks the closed-loop reference system with quantifiable bounds for the state and input. The following theorem shows that the difference between states and inputs of the ℓ_1 controlled system and the closed-loop reference system (27) is bounded.

Theorem 1. For the system in (3) and the controller defined via (4) – (5) and (8) subject to the ℓ_1-norm condition in (9), we have

$$\|x_{ref} - x\|_{\ell_\infty} \leq \gamma_1\,, \quad \|u_{ref} - u\|_{\ell_\infty} \leq \gamma_2\,, \tag{33}$$

where

$$\begin{aligned} \gamma_1 &\triangleq \frac{\|C(z)\|_{\ell_1}}{1 - \|G(z)\|_{\ell_1} L_\theta}\gamma_0\,, \\ \gamma_2 &\triangleq \|H_1(z)\|_{\ell_1}\gamma_0 + \|C(z)\theta^T\|_{\ell_1}\gamma_1\,, \end{aligned} \tag{34}$$

and γ_0 is defined in (11).

Proof. The response of the closed-loop system in (3) with the ℓ_1 adaptive controller in (8) can be written in the z domain as:

$$\begin{aligned} x(z) &= H(z)C(z)k_g r(z) - H(z)C(z)\hat{\eta}(z) + H(z)(\theta^T x(z) + \xi) + x_{in}(z) \\ &= H(z)C(z)k_g r(z) - H(z)C(z)\tilde{\eta}(z) + G(z)(\theta^T x(z) + \xi) + x_{in}(z)\,, \end{aligned} \tag{35}$$

where $H(z)$ and $G(z)$ were defined in (10). The above equality holds because $\tilde{\eta}(z) = \hat{\eta}(z) - \rho^T \begin{bmatrix} x(z) \\ 1 \end{bmatrix}$ and $-\hat{\eta}(z) = -\tilde{\eta}(z) - \rho^T \begin{bmatrix} x(z) \\ 1 \end{bmatrix}$. From the definition of the closed-loop reference system in (27), it follows that

$$x_{ref}(z) = H(z)k_g C(z)r(z) + G(z)\rho^T \begin{bmatrix} x_{ref}(z) \\ 1 \end{bmatrix} + x_{in}(z)\,. \tag{36}$$

The expressions above and the predictor error dynamics in (18) allow us to write

$$\begin{aligned} x_{ref}(z) - x(z) &= G(z)\rho^T \left(\begin{bmatrix} x_{ref}(z) \\ 1 \end{bmatrix} - \begin{bmatrix} x(z) \\ 1 \end{bmatrix} \right) + H(z)C(z)\tilde{\eta}(z) \\ &= G(z)\theta^T(x_{ref}(z) - x(z)) + H(z)C(z)\tilde{\eta}(z) \\ &= G(z)\theta^T(x_{ref}(z) - x(z)) + C(z)\tilde{x}(z)\,, \end{aligned} \tag{37}$$

which implies that

$$\|(x_{ref} - x)|_i\|_{\ell_\infty} \leq \|G(z)\theta^T\|_{\ell_1}\|(x_{ref} - x)|_i\|_{\ell_\infty} + \|C(z)\|_{\ell_1}\|\tilde{x}|_i\|_{\ell_\infty}\,. \tag{38}$$

Then, the bounds in (30) and (24) lead to the following uniform upper bound:

$$\|(x_{ref} - x)|_i\|_{\ell_\infty} \leq \frac{\|C(z)\|_{\ell_1}\|\tilde{x}|_i\|_{\ell_\infty}}{1 - \|G(z)\|_{\ell_1} L_\theta} \leq \frac{\|C(z)\|_{\ell_1}}{1 - \|G(z)\|_{\ell_1} L_\theta}\gamma_0\,. \tag{39}$$

To derive the second bound, notice that (8) and (27) lead to:

$$\begin{aligned} u_{ref}(z) - u(z) &= -C(z)\left(\rho^T \begin{bmatrix} x_{ref}(z) \\ 1 \end{bmatrix} - k_g r(z) \right) + C(z)(\hat{\eta}(z) - k_g r(z)) \\ &= -C(z)\rho^T \begin{bmatrix} x_{ref}(z) \\ 1 \end{bmatrix} + C(z)\hat{\eta}(z) \\ &= -C(z)\theta^T x_{ref}(z) - C(z)\xi + C(z)(\tilde{\eta}(z) + \theta^T x(z) + \xi) \\ &= C(z)\tilde{\eta}(z) - C(z)\theta^T(x_{ref}(z) - x(z))\,. \end{aligned} \tag{40}$$

It follows from the error dynamics in (18) and the definition of $H_1(z)$ in (26) that

$$C(z)\tilde{\eta}(z) = C(z)\frac{c_0^T H(z)}{c_0^T H(z)}\tilde{\eta}(z) = H_1(z)H(z)\tilde{\eta}(z) = H_1(z)\tilde{x}(z)\,, \tag{41}$$

which implies that

$$u_{ref}(z) - u(z) = H_1(z)\tilde{x}(z) - C(z)\theta^T(x_{ref}(z) - x(z))\,, \tag{42}$$

and the following bound holds

$$\|(u_{ref} - u)|_i\|_{\ell_\infty} \leq \|H_1(z)\|_{\ell_1}\|\tilde{x}(z)|_i\|_{\ell_\infty} + \|C(z)\theta^T\|_{\ell_1}\|(x_{ref} - x)|_i\|_{\ell_\infty}\,. \tag{43}$$

This bound holds uniformly. The bounds in (24) and (39) lead to

$$\|(u_{ref} - u)|_i\|_{\ell_\infty} \leq \|H_1(z)\|_{\ell_1}\gamma_0 + \|C(z)\theta^T\|_{\ell_1}\gamma_1 \,. \tag{44}$$

□

In this subsection we used Lemma 5 to show that the closed-loop reference system (27) is BIBS stable. Then, in Theorem 1 we showed that the difference between the state and input of the ℓ_1 controlled system and the state and input of the stable closed-loop reference system is bounded.

3.3 | Performance Bounds

Notice that the LTI closed-loop reference system (27) is not realizable as it depends on knowing the true value of θ and ξ; hence, it cannot be used to describe the ℓ_1 controlled system. In this subsection we show that the ℓ_1 controlled system stays close to a known linear model. Further, we show that the difference between these two systems is bounded.

The ℓ_1 adaptive controller is able to cancel the uncertainties of the system exactly when the uncertainties are within the bandwidth of the low-pass filter. In this *ideal* scenario, the system response is the following:

$$x_{id}(k+1) = A_m x_{id}(k) + b_m k_g r(k) \,, \tag{45}$$

where the subscript x_{id} is used to denote the ideal response. All variables of the ideal system are known; hence, it can be implemented. Next, we show that there exists a uniform upper bound for the difference between the ideal (45) and the ℓ_1 controlled system. This bound will be later used in the robust MPC implementation.

Theorem 2. For the system (3) and the controller defined via (4) – (5) and (8) subject to the ℓ_1-norm condition in (9), we have

$$\|x_{id} - x\|_{\ell_\infty} \leq \|H(z)(1 - C(z)k_g)\|_{\ell_1}\|r\|_{\ell_\infty} + \|H(z)H_1(z)\|_{\ell_1}\gamma_0 + \lambda_\theta\left(\|\hat{x}\|_{\ell_\infty} + \gamma_0\right) + \lambda_\xi \,. \tag{46}$$

Proof. The response of the ideal system in the z domain can be written as:

$$x_{id}(z) = H(z)k_g r(z) + x_{in}(z) \,. \tag{47}$$

The response of the closed-loop system in (3) with the ℓ_1 adaptive controller in (8) can be written in the z domain as (35). The latter implies that:

$$\begin{aligned} x(z) - x_{id}(z) &= H(z)k_g(C(z)-1)r(z) - H(z)C(z)\hat{\eta}(z) + H(z)(\theta^T x(z) + \xi) \\ &= H(z)k_g(C(z)-1)r(z) - H(z)C(z)\tilde{\eta}(z) + G(z)(\theta^T x(z) + \xi) \\ &= H(z)k_g(C(z)-1)r(z) - H(z)H_1(z)\tilde{x}(z) + G(z)(\theta^T x(z) + \xi) \,. \end{aligned} \tag{48}$$

Using the above, the following uniform bound can be derived

$$\begin{aligned} \|(x - x_{id})|_i\|_{\ell_\infty} \leq \|H(z)k_g(C(z)-1)\|_{\ell_1}\|r|_i\|_{\ell_\infty} + \|H(z)H_1(z)\|_{\ell_1}\gamma_0 \\ + \lambda_\theta\left(\|\hat{x}\|_{\ell_\infty} + \|\tilde{x}\|_{\ell_\infty}\right) + \lambda_\xi \,, \end{aligned} \tag{49}$$

where γ_0 was defined in (11) and $\|\hat{x}\|_{\ell_\infty}$ was defined in (25). □

Ideally, the controller would be able to compensate for all the unknown parameters in the system, which would make the controlled system behave exactly as the ideal system (45). However, this is not always possible and modeling errors arise. In Theorem 2, we showed that there exists a uniform upper bound for the difference between the real and the ideal system. This bound can be interpreted as a bound on the modeling error of the adaptive system by the linear model (45), which is required for the implementation of the robust MPC, as will be shown in the next section.

4 | ROBUST MODEL PREDICTIVE CONTROL

In the nominal implementation of MPC, it is difficult to incorporate plant model uncertainties explicitly [44] and to guarantee robust stability of the origin. Robust MPC implementations are able to account for the above, but require a bound on the disturbance in

the system, which may be thought of as a modeling error. In section 3, we presented a discrete-time state feedback ℓ_1 adaptive controller that is able to provide a system model and an upper bound on the modeling error. For the framework proposed in this paper, any robust MPC implementation that has a bounded additive disturbance[22,23] can be used. In this work we use the robust MPC for linear systems with additive disturbance proposed in[22]. For convenience and completeness, we briefly describe the robust MPC approach. The discrete-time system with additive disturbances to be controlled by the robust MPC is described by

$$x(k+1) = A_m x(k) + b_m u(k) + w\,, \tag{50}$$

where $x(k) \in \mathbb{R}^n$ is the state at time step k, $u \in \mathbb{R}$ is the input, $w \in \mathbb{R}^n$ is a bounded disturbance, and $x(k+1)$ denotes the successor state. The system is subject to state and input constraints

$$u \in \mathbb{U}\,, \quad x \in \mathbb{X}\,, \tag{51}$$

where $\mathbb{U} \subset \mathbb{R}$ is compact, $\mathbb{X} \subset \mathbb{R}^n$ is closed, and each set contains the origin in its interior. We further assume that $\mathbb{U}$ and $\mathbb{X}$ are polytopic. The disturbance is given by

$$w \in W\,, \tag{52}$$

where W is compact, polytopic, and contains the origin. Let $\mathbf{u} = [u(0), \dots, u(H-1)]$ be the control sequence and $\mathbf{w} = [w(0), \dots, w(H-1)]$ be the disturbance sequence, where H is the RMPC time horizon. Let $\phi(k; x, \mathbf{u}, \mathbf{w})$ be the solution of (50) at time k when the initial state is x (at time 0) and the control and disturbance sequences are $\mathbf{u}$ and $\mathbf{w}$, respectively. We define the *nominal* system corresponding to (50) as

$$\bar{x}(k+1) = A_m \bar{x}(k) + b_m \bar{u}(k)\,, \tag{53}$$

and define $\bar{\phi}(k; \bar{x}, \bar{\mathbf{u}})$ as the solution of (53) at time k when the initial state is $\bar{x}$ and the control sequence is $\bar{\mathbf{u}} = [\bar{u}(0), \dots, \bar{u}(H-1)]$.

Let $K \in \mathbb{R}^{m \times n}$ be such that $A_K \triangleq A_m + b_m K$ is stable. Further, let Z be a disturbance invariant set for the controlled uncertain system $x(k+1) = A_K x(k) + w$ satisfying

$$A_K Z \oplus W \subseteq Z\,, \tag{54}$$

where $\oplus$ denotes Minkowski set addition, i.e., $A \oplus B \triangleq \{a+b \mid a \in A, b \in B\}$. The set Z serves as the 'origin' for the perturbed system. In order to reduce conservativeness, the set Z should be as small as possible. Different ways to calculate and minimize Z are presented in[22]. We follow[45] to compute Z as a polytopic, disturbance invariant, outer approximation of the minimal robust positively invariant set. The following Proposition is introduced as it is required for the definition of the controller. It states that the feedback policy $u(k) = \bar{u}(k) + K(x(k) - \bar{x}(k))$ keeps the states $x(k)$ of the uncertain system (50) close to the states $\bar{x}(k)$ of the nominal system (53) for all $\bar{u}(\cdot)$, $x(k) \in \bar{x}(k) \oplus Z$ if $x(0) \in \bar{x}(0) \oplus Z$.

Proposition 1. Suppose Z is disturbance invariant for $x(k+1) = A_K x(k) + w$. If $x(k) \in \bar{x}(k) \oplus Z$ and $u(k) = \bar{u}(k) + K(x(k) - \bar{x}(k))$, then $x(k+1) \in \bar{x}(k+1) \oplus Z$ for all $w \in W$ where $x(k+1) = A_m x(k) + b_m u(k) + w$ and $\bar{x}(k+1) = A_m \bar{x}(k) + b_m \bar{u}(k)$.

The robust MPC used in this work[22] has three main changes compared to nominal MPC *(i)* addition of the initial state as a decision variable, *(ii)* tightening of state and input constraints, and *(iii)* modification of the control law to include an ancillary controller. Recall that when there are additive disturbances, it may not be true that the cost function decreases for the next step[22] for all disturbances affecting the system. Moreover, the set Z is invariant under state feedback with gain K. Hence, we need to establish robust asymptotic stability of Z. To do this, the optimization problem incorporates the initial state. This is possible as the initial state x_0 in the optimal control problem is not the current state $x(k)$ of a plant, but a parameter of the control law. The problem $\mathbb{P}_H^*(x(k))$ for the robust MPC is defined as follows

$$V_H^*(x(k)) = \min_{x_0, \mathbf{u}} \{V_H(x_0, \mathbf{u}) \mid \mathbf{u} \in \mathcal{U}_H(x_0),\ x(k) \in x_0 \oplus Z\}\,, \tag{55}$$

$$(x_0^*(x(k)), \mathbf{u}^*(x(k))) = \arg\min_{x_0, \mathbf{u}} \{V_H(x_0, \mathbf{u}) \mid \mathbf{u} \in \mathcal{U}_H(x_0),\ x(k) \in x_0 \oplus Z\}\,, \tag{56}$$

where the cost function $V_H(\cdot)$ is defined over the time horizon H by

$$V_H(x(k), \mathbf{u}) \triangleq \sum_{i=0}^{H-1} l(x(i), u(i)) + V_f(x(H))\,, \tag{57}$$

where the stage cost l and terminal cost V_f are defined as

$$l(x, u) \triangleq x^T Q_{\mathrm{MPC}} x + u^T R_{\mathrm{MPC}} u\,, \quad V_f(x) \triangleq x^T P_{\mathrm{MPC}} x\,, \tag{58}$$

and Q_{MPC}, R_{MPC} and P_{MPC} are positive definite. Note that the problem $\mathbb{P}_H^*(x(k))$ incorporates the initial state as a decision variable. Moreover, $\mathcal{U}_H x(k)$ is the set of control sequences satisfying the tighter control, state and terminal constraints defined by

$$\begin{aligned} &u(i) \in \bar{\mathbb{U}} \triangleq \mathbb{U} \ominus K Z\,, \quad i \in \mathcal{I}_{H-1}\,,\\ &x(i) \in \bar{\mathbb{X}} \triangleq \mathbb{X} \ominus Z\,, \quad i \in \mathcal{I}_{H-1}\,,\\ &x(H) \in \bar{\mathbb{X}}_f \subset \mathbb{X} \ominus Z\,, \end{aligned} \tag{59}$$

where $\mathcal{I}_{H-1} \triangleq \{0, 1, \dots, H-1\}$, and $\bar{\mathbb{X}}_f$ is the terminal constraint set for $\mathbb{P}_H^*(x(k))$, which is assumed to have a non-empty interior. We choose $\bar{\mathbb{X}}_f$ as the maximal robust positively invariant set, which is polytopic due to the polytopic input and state constraints, and compute it following[46] for the tightened input and state constraints. Note that the minimal Z is proportional to W. Therefore, we assume that the set W is small enough to ensure that $Z \subset$ interior($\mathbb{X}$) and $KZ \subset$ interior($\mathbb{U}$). Hence, the set of input sequences satisfying the tighter input, state, and terminal constraints is given by

$$\mathcal{U}_H(x) = \{\mathbf{u} \mid u(i) \in \bar{\mathbb{U}},\, \bar{\phi}(i; x, \mathbf{u}) \in \bar{\mathbb{X}},\, \forall i \in \mathcal{I}_{H-1},\, \bar{\phi}(H; x, \mathbf{u}) \in \bar{\mathbb{X}}_f\}\,, \tag{60}$$

where $x(i) = \bar{\phi}(i; x, \mathbf{u})$.

The initial state $x_{\underline{0}}$ of the model is a decision variable that can be varied if it satisfies the following constraint

$$x(k) \in x_{\underline{0}} \oplus Z\,, \tag{61}$$

where $x(k)$ is the current state of the system being controlled. It can be shown that $\mathbb{P}_H^*(x(k))$ is a quadratic program (QP) that yields the optimal control sequence $\mathbf{u}^*(x(k)) \triangleq \{u_0^*(x(k)), \dots, u_{H-1}^*(x(k))\}$ and the optimal state sequence $\mathbf{x}^*(x(k)) \triangleq \{x_{\underline{0}}^*(x(k)), \dots, x_H^*(x(k))\}$ where, for each $i > 0$, $x_i^*(x(k)) \triangleq \bar{\phi}(i; x_{\underline{0}}^*(x(k)), \mathbf{u}^*(x(k)))$. Note that the optimal state $x_{\underline{0}}^*(x(k))$ is not necessarily equal to the current state $x(k)$. A pair $(x_{\underline{0}}, \mathbf{u})$ is a feasible solution of $\mathbb{P}_H^*(x(k))$ if $x(k) \in x_{\underline{0}} \oplus Z$ and $\mathbf{u} \in \mathcal{U}_H(x_{\underline{0}})$. We propose the following implicit model predictive control law $\kappa_H^*(\cdot)$, yielded by the solution of $\mathbb{P}_H^*(x(k))$

$$\kappa_H^*(x(k)) \triangleq u_0^*(x(k)) + K(x(k) - x_{\underline{0}}^*(x(k)))\,. \tag{62}$$

The control $\kappa_H^*(x(k))$ is not necessarily equal to $u_0^*(x(k))$, as in conventional model predictive control. Let $x(k)$ be an arbitrary state in

$$X_H \triangleq \{x \mid \exists\, x_{\underline{0}} \text{ such that } x(k) \in x_{\underline{0}} \oplus Z,\, \mathcal{U}_H(x_{\underline{0}}) \neq \emptyset\}\,, \tag{63}$$

the domain of the value function $V_H^*(\cdot)$. The optimal control and state trajectories for the problem $\mathbb{P}_H^*(x(k))$, $\mathbf{u}^*(x(k))$ and $\mathbf{x}^*(x(k))$, respectively, satisfy

$$\begin{aligned} &u_i^*(x(k)) \in \mathbb{U} \ominus K Z\,,\\ &x_i^*(x(k)) \in \mathbb{X} \ominus Z\,, \forall i \in \mathcal{I}_{H-1} \text{ and}\\ &x_H^*(x(k)) \in \bar{\mathbb{X}}_f \subset \mathbb{X} \ominus Z\,. \end{aligned} \tag{64}$$

In[22] it was shown that for the above robust model predictive controller, the set Z is robustly exponentially stable for the controlled uncertain system $x(k+1) = A_m x(k) + b_m \kappa_{N_H}^*(x(k)) + w$ where $w \in W$, and that the region of attraction is X_H.

Finally, we can write the constrained finite-time optimal control (CFTOC) problem to be solved for RMPC at time step k as

$$V_H^*(x(k)) = \min_{\mathbf{x},\mathbf{u}} \quad \sum_{i=0}^{H-1} l(x_i, u_i) + V_f(x_H) \tag{65a}$$

$$\text{s.t.} \quad x_{i+1} = A_m x_i + b_m u_i\,, \forall i \in \mathcal{I}_{H-1} \tag{65b}$$

$$x_i \in \bar{\mathbb{X}}\,, \forall i \in \mathcal{I}_H \tag{65c}$$

$$u_i \in \bar{\mathbb{U}}\,, \forall i \in \mathcal{I}_{H-1} \tag{65d}$$

$$x_H \in \bar{\mathbb{X}}_f \tag{65e}$$

$$x(k) \in x_{\underline{0}} \oplus Z\,. \tag{65f}$$

The first input from the obtained optimal control sequence $\mathbf{u}^*(x(k))$ is then passed to (62) and the resulting control $\kappa_H^*(x(k))$ is applied to the system (50). This procedure is repeated for all following time steps in a receding horizon manner.

5 | ROBUST ADAPTIVE MPC FRAMEWORK

This section presents the proposed robust adaptive MPC framework (see Fig. 1), which yields the RMPC-$\mathscr{L}_1$ controller. We propose an $\mathscr{L}_1$ adaptive controller (orange dashed box in Fig. 1) as an underlying controller to a robust MPC (blue box in Fig. 1) to achieve low-cost and accurate stabilization to the origin of a system with parametric uncertainties and state and input constraints. The key idea of this framework is to leverage characteristics of the discrete-time state feedback $\mathscr{L}_1$ adaptive controller to satisfy the requirements for the linear robust MPC and vice versa.

In section 3 we showed that the proposed discrete-time state feedback $\mathscr{L}_1$ adaptive controller is able to make a system behave close to an ideal linear system (45). The ideal system behavior is achievable only if all the uncertainties in the system are canceled, which is not always attainable. Therefore, the behavior of the controlled system may deviate from the ideal system behavior. We showed that the deviation between ideal and $\mathscr{L}_1$ controlled system behavior is bounded (46) and can be thought of as a bound on the modeling error. We can then reformulate the ideal linear system (45) as a linear system with the bounded additive disturbance (46) as:

$$x(k+1) = A_m x(k) + b_{\mathscr{L}_1} u(k) + w\,, \tag{66}$$

where $b_{\mathscr{L}_1} \triangleq b_m k_g$, k_g is defined in section 3.1 and $x \in \mathbb{X}$, $u \in \mathbb{U}$ as in (51) and $w \in W_{\mathscr{L}_1}$. In this work, the additive disturbance set $W_{\mathscr{L}_1}$ is approximated by an outer bounding box on the modeling error specified by (46). We note that the existence of the bound on the modeling error (46) requires a bounded initial state x_0 and a bounded reference $r(k)$, which is computed by the RMPC, as shown in Fig. 1. In our proposed robust adaptive MPC the initial condition x_0 and the reference are constrained by the bounded sets $\mathbb{X}$ and $\mathbb{U}$, respectively. Therefore, the bound on the modeling error (46) exists and can be obtained.

In section 4 we described a robust MPC for linear systems with bounded additive disturbances of the form (66). In contrast to the RMPC formulation, the RMPC-$\mathscr{L}_1$ uses the input matrix $b_{\mathscr{L}_1}$ and the disturbance set $W_{\mathscr{L}_1}$. In general, this requires a different choice for the stabilizing state feedback gain, that we denote as $K_{\mathscr{L}_1}$, and the terminal cost function, which we define as

$$V_{f,\,\mathscr{L}_1}(x) = x^T P_{\text{MPC},\,\mathscr{L}_1} x\,. \tag{67}$$

Following[45] we determine the disturbance invariant set $Z_{\mathscr{L}_1}$ as a polytopic approximation for system (66) with A_m, $b_{\mathscr{L}_1}$, $K_{\mathscr{L}_1}$ and $W_{\mathscr{L}_1}$. Alternatively, we can also directly use the modeling error (46) as an over-approximation of an RPI set for constraint tightenting and remove the optimization over the initial state in the RMPC formulation for recursive feasibility[47]. Tightening the state and input constraints using the disturbance invariant set $Z_{\mathscr{L}_1}$ yields $\bar{\mathbb{X}}_{\mathscr{L}_1}$ and $\bar{\mathbb{U}}_{\mathscr{L}_1}$. Then we obtain the terminal set $\bar{\mathbb{X}}_{f,\,\mathscr{L}_1}$ as the maximal robust positively invariant set for the tightened $\bar{\mathbb{X}}_{\mathscr{L}_1}$ and $\bar{\mathbb{U}}_{\mathscr{L}_1}$ and the gain $K_{\mathscr{L}_1}$ for system (66). After defining all the necessary sets, the terminal cost and the feedback gain for the proposed robust adaptive MPC, we can write the CFTOC problem to be solved at time k as

$$V^*_{H,\,\mathscr{L}_1}(x(k)) = \min_{\mathbf{x}_{\mathscr{L}_1},\mathbf{u}_{\mathscr{L}_1}} \quad \sum_{i=0}^{H-1} l(x_{i,\,\mathscr{L}_1}, u_{i,\,\mathscr{L}_1}) + V_{f,\,\mathscr{L}_1}(x_{H,\,\mathscr{L}_1}) \tag{68a}$$

$$\text{s.t.} \quad x_{i+1,\mathscr{L}_1} = A_m x_{i,\,\mathscr{L}_1} + b_{\mathscr{L}_1} u_{i,\,\mathscr{L}_1}\,, \forall i \in \mathcal{I}_{H-1} \tag{68b}$$

$$x_{i,\,\mathscr{L}_1} \in \bar{\mathbb{X}}_{\mathscr{L}_1}\,, \forall i \in \mathcal{I}_H \tag{68c}$$

$$u_{i,\,\mathscr{L}_1} \in \bar{\mathbb{U}}_{\mathscr{L}_1}\,, \forall i \in \mathcal{I}_{H-1} \tag{68d}$$

$$x_{H,\,\mathscr{L}_1} \in \bar{\mathbb{X}}_{f,\,\mathscr{L}_1} \tag{68e}$$

$$x(k) \in x_{0,\,\mathscr{L}_1} \oplus Z_{\mathscr{L}_1}\,. \tag{68f}$$

The solution to the CFTOC yields the optimal control input sequence

$$\mathbf{u}^*_{\mathscr{L}_1}(x(k)) = \left[u^*_{0,\mathscr{L}_1}(x(k)), \dots, u^*_{H-1,\mathscr{L}_1}(x(k))\right]\,, \tag{69}$$

where the first element of the optimal control input sequence $u^*_{0,\mathscr{L}_1}(x(k))$ is used inside the ancillary controller

$$\kappa^*_{H,\,\mathscr{L}_1}(x(k)) \triangleq u^*_{0,\,\mathscr{L}_1}(x(k)) + K_{\mathscr{L}_1}(x(k) - x^*_{0,\,\mathscr{L}_1}(x(k)))\,. \tag{70}$$

This input is used as the reference signal $r(k)$ for the underlying $\mathscr{L}_1$ adaptive controller. The above CFTOC for the robust adaptive MPC is solved again at the next time step with the initial state $x(k+1)$ and the next reference to the underlying $\mathscr{L}_1$ AC is provided. This is repeated for all time steps in a receding horizon fashion. Moreover, since the robust MPC is able to handle input and state constraints, it can guarantee that the states and references to the $\mathscr{L}_1$ controlled system are constrained to sets where the bound (46) holds. In summary, the underlying $\mathscr{L}_1$ adaptive controller is able to provide a linear system model with bounded

additive disturbances to be used by the RMPC; while the RMPC provides the $\mathscr{l}_1$ adaptive controller with a reference signal that lies within the bounds that make the bound (46) hold. In this way, we achieve stabilization in the presence of modeling errors.

The proposed approach has been formulated for SISO systems with constant matched disturbances. As stated above, the system has to satisfy the assumptions of the $\mathscr{l}_1$ adaptive controller and the RMPC. In particular, *(i)* the $\mathscr{l}_1$ adaptive controller must provide a bound for the difference between the behavior of the ideal system and the $\mathscr{l}_1$ controlled system, *(ii)* the ideal system should be a linear system with an additive disturbance (50), and *(iii)* the RMPC must be able to satisfy the input constraint of the $\mathscr{l}_1$ controlled system. Therefore, it is possible to extend this approach to MIMO systems with time-varying matched and unmatched uncertainties if an appropriately designed underlying $\mathscr{l}_1$ adaptive controller is able to provide a bound for the difference between the behavior of the ideal system and the $\mathscr{l}_1$ controlled system.

6 | ILLUSTRATIVE EXAMPLE

This section presents a numerical example for the proposed robust adaptive MPC. We assess the proposed framework with respect to three metrics: *(i)* feasibility, *(ii)* performance, and *(iii)* accuracy of the stabilization task. In order to do this, we compare the performance of the proposed framework (RMPC-$\mathscr{l}_1$) to the performance of the following baseline controllers: *(i)* Linear Quadratic Regulator (LQR), *(ii)* nominal MPC (MPC), *(iii)* robust MPC (RMPC), *(iv)* LQR with underlying $\mathscr{l}_1$ adaptive control (LQR-$\mathscr{l}_1$), *(v)* MPC with underlying $\mathscr{l}_1$ adaptive control (MPC-$\mathscr{l}_1$), and *(vi)* $\mathscr{l}_1$ adaptive control ($\mathscr{l}_1$ AC).

The proposed and baseline controllers are used to stabilize the constrained system defined by

$$\begin{aligned} \underbrace{\begin{bmatrix} x_1(k+1) \\ x_2(k+1) \end{bmatrix}}_{x(k+1)} &= \underbrace{\begin{bmatrix} 1 & 0.5 \\ -0.5 & -0.2 \end{bmatrix}}_{A} \underbrace{\begin{bmatrix} x_1(k) \\ x_2(k) \end{bmatrix}}_{x(k)} + \underbrace{\begin{bmatrix} 0.5 \\ 0.5 \end{bmatrix}}_{b_m} (u(k) + \theta^T x(k) + \xi), \\ y(k) &= \underbrace{\begin{bmatrix} 1 & 0 \end{bmatrix}}_{c_m^T} x(k), \end{aligned} \tag{71}$$

where $\theta = \begin{bmatrix} \theta_1 & \theta_2 \end{bmatrix}^T$. For this example, we consider a stable system and set $k_m = \begin{bmatrix} 0 & 0 \end{bmatrix}^T$, which yields $A_m = A$. The state constraints are $x \in \mathbb{X} \triangleq \left\{ x \in \mathbb{R}^2 \mid |x_1| \leq 5,\ |x_2| \leq 2 \right\}$; and the input constraint is $u \in \mathbb{U} \triangleq \{u \in \mathbb{R} \mid |u| \leq 5\}$. The unknown parameters lie in $\theta \in \Theta \triangleq \left\{ \theta \in \mathbb{R}^2 \mid \|\theta\|_\infty \leq 0.05 \right\}$ and $\xi \in \Xi \triangleq \{\xi \in \mathbb{R} \mid |\xi| \leq 0.2\}$. In the experiments we use the following values for the unknown parameters $\theta = [-0.0425,\ -0.0425]^T$ and $\xi = -0.175$.

In this section we first provide details on the implementation of the proposed and baseline controllers. Then, we will specify the metrics we use to compare the controllers in the next section. Finally, we show numerical results comparing the different controllers according to the defined metrics.

6.1 | Proposed and Baseline Control Implementation

In this section we present implementation details of the proposed controller and the six baseline controllers. We begin by describing the implementation of the $\mathscr{l}_1$ adaptive controller. The $\mathscr{l}_1$ adaptive controller is defined in equations (4), (5), and (8) For this numerical example, we choose $C(z)$ as a first-order, low-pass filter of the form:

$$C(z) = \frac{\omega_{\mathscr{l}_1}}{1 + (\omega_{\mathscr{l}_1} - 1)z^{-1}},$$

where $\omega_{\mathscr{l}_1} = 0.95$. One of the main restrictions posed in Assumption 2 is the satisfaction of the inequality $(e^{\tau\rho_{\max}} - 1)4nc_1^2 < 2$. With this choice of $\omega_{\mathscr{l}_1}$, the latter inequality is satisfied since $(e^{\tau\rho_{\max}} - 1)4nc_1^2 = 0.0021$. Moreover, we initialize the adaptive parameter as $\hat{\rho}_0 = [0, 0, 0]^T$.

The baseline controllers consist of optimization-based controllers with (see Fig. 2) and without (see Fig. 3) an underlying $\mathscr{l}_1$ adaptive controller. In the following we show that the implementation of the optimization-based controllers depends on the presence or absence of an underlying $\mathscr{l}_1$ adaptive controller. The $\mathscr{l}_1$ adaptive controller makes the system behave close to an ideal system of the form (45). We consider that the ideal system has an additive disturbance as in (66) since there exists a bounded difference between the behavior of the $\mathscr{l}_1$ controlled system and the behavior of the ideal system. Using the numerical values

of (71), we can rewrite (66) as

$$x(k+1) = \underbrace{\begin{bmatrix} 1 & 0.5 \\ -0.5 & -0.2 \end{bmatrix}}_{A_m} x(k) + \underbrace{\begin{bmatrix} 0.1470 \\ 0.1470 \end{bmatrix}}_{b_{\ell_1}} u(k) + w\,. \tag{72}$$

where $w \in W_{\ell_1}$. In this work we approximate W_{ℓ_1} through experiments using system (71) with an underlying ℓ_1 adaptive controller since the bound computed with (46) is too conservative. For this numerical example, three out of the four terms to the right of (46) (without $\|H(z)H_1(z)\|_{\ell_1}\gamma_0$) add up to 0.7922, which would yield a tightened constrained state set $\bar{\mathbb{X}}$ that is overly conservative (compared to the tightened constrained state set $\bar{\mathbb{X}}$ that is calculated below using the disturbance invariant set Z_{ℓ_1}). Notice that the bound (46) depends on the system matrices A_m, b_m, the chosen low-pass filter $C(z)$, the ℓ_∞-norm of the reference signal, the bounds on the parameter sets Θ, Ξ, and the initial state of the system. Moreover, we have state $\mathbb{X}$ and input $\mathbb{U}$ constraints for this problem. Therefore, we estimate W_{ℓ_1} from experiments by *(i)* setting the initial state x_0 as each of the vertices of $\mathbb{X}$, *(ii)* setting the reference $r(k)$ as a step function where the step size is as large as possible while satisfying the input constraint, i.e., $r(k) = 5$ and $r(k) = -5$ for $k > 1$, and *(iii)* setting θ and ξ with values at the boundary of the parameter sets Θ, Ξ. For each experiment i, the maximum disturbance value $w_{i,max}$ is calculated as the difference between the actual next state $x(k+1)$ obtained in the experiments and the undisturbed next state $x_{id}(k+1)$ calculated using (72) with $w = 0$ and $x_{id}(k) = x(k)$. Finally, we find the maximum disturbance encountered in all the experiments w_{max} and set $W_{\ell_1} \triangleq \{w \in \mathbb{R}^2 \mid \|w\|_\infty \leq 0.3118\}$ for this numerical example. For systems without an underlying ℓ_1 adaptive controller, it is convenient to rewrite (71) to match the form of (50), with the parametric uncertainties lumped in w. For this numerical example, (71) can be rewritten as

$$x(k+1) = \underbrace{\begin{bmatrix} 1 & 0.5 \\ -0.5 & -0.2 \end{bmatrix}}_{A_m} x(k) + \underbrace{\begin{bmatrix} 0.5 \\ 0.5 \end{bmatrix}}_{b_m} u(k) + w\,, \tag{73}$$

where $w \in W$, and W can be calculated given the state constraints, bounds on the unknown parameters, and b_m. In this work, we approximate W as the difference between the true (disturbed) system (50) and the undisturbed system (where $\theta, \xi = 0$). Then the disturbance set W is the outer bounding box approximation of $\bar{W}$, which is determined from the known parameter sets Θ and Ξ by

$$\bar{W} = \bigcup_{v \,\in\, \text{extreme}(\Theta)} b_m(v^T\mathbb{X} \oplus \Xi)\,, \tag{74}$$

where extreme(Θ) denotes the set of vertices of Θ. For this numerical example, the set W is defined by $w \in W \triangleq \{w \in \mathbb{R}^2 \mid \|w\|_\infty \leq 0.275\}$.

In the next calculations we use b_{ℓ_1} for controllers with an underlying ℓ_1 adaptive controller (Fig. 2), and b_m for controllers without an underlying ℓ_1 adaptive controller (Fig. 3).

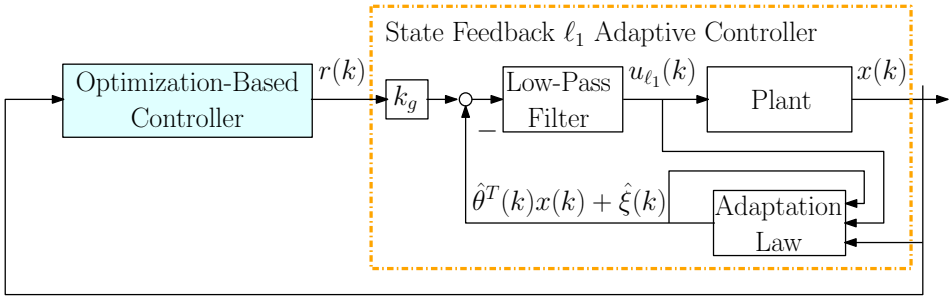

FIGURE 2 Architecture of baseline controllers with an underlying ℓ_1 adaptive control.

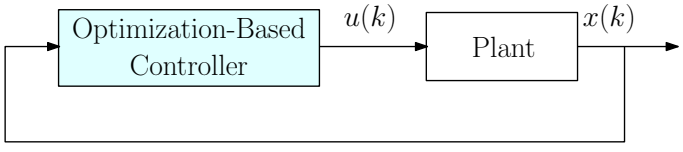

FIGURE 3 Architecture of baseline controllers without an underlying ℓ_1 adaptive control.

Next, we give implementation details of the baseline controllers LQR and LQR-ℓ_1. The infinite-horizon discrete-time LQR cost function has the following weights:

$$Q = \begin{bmatrix} 1 & 0 \\ 0 & 0.1 \end{bmatrix}, \quad R = 0.055\,. \tag{75}$$

Using the above weights and the nominal ($w = 0$) versions of systems (73) and (72) we can calculate the following LQR gains $K_{\text{LQR}} = [-1.2846,\ -0.6592]$ and $K_{\text{LQR},\,\ell_1} = [-2.3313,\ -1.2108]$ for the LQR and LQR-ℓ_1 approach, respectively. For the LQR-ℓ_1 approach, the input calculated with the $K_{\text{LQR},\,\ell_1}$ gain is passed to the ℓ_1 adaptive controller as reference signal.

In the following we present implementation details for the baseline controllers MPC and MPC-ℓ_1. The cost function for the nominal MPC uses the weights in (75). Recall that the terminal cost has a weight P, which is the value function for the nominal ($w = 0$) versions of systems (73) and (72) for the MPC and MPC-ℓ_1 approach, respectively. The P_{MPC} and $P_{\text{MPC},\,\ell_1}$ values are:

$$P_{\text{MPC}} = \begin{bmatrix} 1.3625 & 0.1739 \\ 0.1739 & 0.1835 \end{bmatrix}, \quad P_{\text{MPC},\,\ell_1} = \begin{bmatrix} 1.8490 & 0.4253 \\ 0.4253 & 0.3135 \end{bmatrix}. \tag{76}$$

Moreover, the state an input constraints used for MPC and MPC-ℓ_1 are $\mathbb{X}$ and $\mathbb{U}$, which are not tightened by a disturbance invariant set. The nominal MPC implementation does not consider the initial state as a decision variable. Further, the terminal sets $\mathbb{X}_f$ for MPC and $\mathbb{X}_{f,\,\ell_1}$ for MPC-ℓ_1 are determined according to[46] using the nominal state and input constraints $\mathbb{X}$ and $\mathbb{U}$ with the appropriate system matrices (73) and (72) and LQR gains obtained above. Note that the terminal set $\mathbb{X}_f$ for MPC is a control invariant set for the nominal ($w = 0$) version of system (73) under state feedback with gain K_{LQR}. The same holds for the case with an underlying ℓ_1 AC. For the MPC-ℓ_1 approach, the first element of the optimal input sequence obtained by solving the CFTOC is passed to the ℓ_1 adaptive controller as reference signal $r(k)$.

Similar to the nominal MPC implementations we use the weights in (75) and (76) for RMPC and the proposed RMPC-ℓ_1. In this work, the ancillary controller gains K and K_{ℓ_1} are computed as the state feedback gains K_{LQR} and $K_{\text{LQR},\,\ell_1}$, respectively, which we calculated above. We determine the disturbance invariant set Z for RMPC as a polytopic approximation for system (73) using the procedure described in[45] and with A_m, b_m, K and W. Similarly we obtain the disturbance invariant set Z_{ℓ_1} for RMPC-ℓ_1 as a polytopic approximation for system (72) using A_m, b_{ℓ_1}, K_{ℓ_1} and W_{ℓ_1}. Finally, we calculate the tightened state $\bar{\mathbb{X}}$ and input $\bar{\mathbb{U}}$ constraints according to (59).

We run the controllers for $N = 15$ time steps, while the MPC-based controllers have a horizon $H = 9$, which is chosen such that the system reaches the terminal set in H steps and the origin in the remaining $N - H$ steps. Finally, we compute the sets presented in this paper with the Multi-Parametric Toolbox[48]. Then we solve the CFTOC problems for the MPC, MPC-ℓ_1, RMPC, and RMPC-ℓ_1 as a QP without substitution[49] at every time step using CVXOPT[50].

7 | EVALUATION FRAMEWORK

This section introduces the three metrics that are employed to compare the different controllers: *(i)* feasibility, *(ii)* performance measured by the cost, and *(iii)* accuracy of a stabilization task.

7.1 | Feasibility

In the following we describe how we determine and evaluate the feasibility for the different controllers. In general, all the feasible initial conditions for which admissible control sequences exist form a controllable set. Controllers with larger controllable sets have more feasible initial conditions. Therefore, we compare controllable set sizes.

First, we describe the construction of the robust controllable sets for the RMPC and RMPC-ℓ_1 aproaches. For these predictive controllers the robust controllable sets are defined with respect to the prediction horizon H. The H-step robust controllable sets $\mathbb{K}_H(\mathbb{S})$ and $\mathbb{K}_{H,\,\ell_1}(\mathbb{S})$ for systems (73) and (72), respectively, evolve the system to the target set $\mathbb{S}$ in H steps, without violating state or input constraints for all realizations of the disturbances[49]. Following the tube-based RMPC approach, we obtain the H-step robust controllable sets for systems (73) and (72) in two steps. In the first step, we calculate the j-step robust controllable sets $\bar{\mathbb{K}}_j(\mathbb{S})$ and $\bar{\mathbb{K}}_{j,\,\ell_1}(\mathbb{S})$, $\forall j \in \mathcal{I}_H$, using the tightened state and input constraints ($\bar{\mathbb{X}}$, $\bar{\mathbb{U}}$ for the RMPC and $\bar{\mathbb{X}}_{\ell_1}$, $\bar{\mathbb{U}}_{\ell_1}$ for the RMPC-ℓ_1 approach) through the recursive formula[49] as follows

$$\begin{aligned} &\bar{\mathbb{K}}_j(\mathbb{S}) = \text{Pre}(\bar{\mathbb{K}}_{j-1}(\mathbb{S})) \cap \bar{\mathbb{X}}\,, \quad \bar{\mathbb{K}}_0(\mathbb{S}) = \mathbb{S}\,, \\ &\bar{\mathbb{K}}_{j,\,\ell_1}(\mathbb{S}) = \text{Pre}(\bar{\mathbb{K}}_{j-1,\,\ell_1}(\mathbb{S})) \cap \bar{\mathbb{X}}_{\ell_1}\,, \quad \bar{\mathbb{K}}_{0,\,\ell_1}(\mathbb{S}) = \mathbb{S}\,, \quad j \in \mathcal{I}_H \setminus \{0\}\,, \end{aligned} \tag{77}$$

where Pre(·) is the precursor or one-step backward-reachable set. We specify the target set $\mathbb{S}$ as the terminal sets $\bar{\mathbb{X}}_f$ and $\bar{\mathbb{X}}_{f,\ell_1}$ for the RMPC and RMPC-ℓ_1 approaches, respectively. In the second step, we offset the robust controllable sets at step H by the corresponding disturbance invariant set (Z for the RMPC and Z_{ℓ_1} for the RMPC-ℓ_1 approach) as follows

$$\mathbb{K}_H(\mathbb{S}, Z) = \bar{\mathbb{K}}_H(\mathbb{S}) \oplus Z\,, \quad \mathbb{K}_{H,\ell_1}(\mathbb{S}, Z_{\ell_1}) = \bar{\mathbb{K}}_{H,\ell_1}(\mathbb{S}) \oplus Z_{\ell_1}\,. \tag{78}$$

Initial states inside the H-step robust controllable sets have guaranteed feasibility of the CFTOC over the prediction horizon.

Second, we note that the terminal sets for LQR and LQR-ℓ_1 and the H-step controllable sets for MPC and MPC-ℓ_1 are inaccurate due to the unaccounted disturbance w in the controllers, which renders the method above inapplicable for these cases. Therefore, we use an outer approximation of the N-step controllable sets for LQR, MPC, ℓ_1 AC, LQR-ℓ_1, and MPC-ℓ_1 obtained from simulations, where the target set is the origin. A state is feasible (belongs to the N-step controllable set) if the state and input constraints are satisfied for the N steps even if there is a steady-state error at step N. For the simulations we consider the discrete state space grid $\mathbb{X}_\delta = \{x_1 + j\delta | \forall j \in \mathbb{Z}\} \times \cdots \times \{x_n + j\delta | \forall j \in \mathbb{Z}\} \cap \mathbb{X}$, where $x \in \mathbb{R}^n$, $\delta > 0$, and $\mathbb{Z}$ is the set of integers. The set of simulated feasible initial conditions is defined as $\mathbb{X}_{N,\delta} \subset \mathbb{X}_\delta$. The N-step controllable set is approximated by offsetting the convex hull of $\mathbb{X}_{N,\delta}$ by the discretization δ

$$\mathbb{K}_{N,\delta} = \text{conv}(\mathbb{X}_{N,\delta}) \oplus \mathbb{B}(\delta) \cap \mathbb{X}\,, \tag{79}$$

where $\mathbb{B}(\delta)$ is a ball with radius δ. This yields the outer approximation of the true N-step controllable set $\mathbb{K}_N \subset \mathbb{K}_{N,\delta}$. In experiments the N-step controllable sets for LQR, MPC, ℓ_1, LQR-ℓ_1, and MPC-ℓ_1 are approximated using $\delta = 0.05$.

7.2 | Performance

Performance is the ability of a controller to minimize a user-specified quadratic control objective. The quadratic form of the cost function allows the comparison of the controllers according to cost function sublevel sets for chosen sublevels $\zeta > 0$, since the sublevels are necessarily convex. We use the quadratic cost function (58) with weights specified in (75) and the sequence of visited states $\mathbf{x}(x_0) = \left[x_0\,, x(1)\,, \dots\,, x(N)\right]$ and applied inputs $\mathbf{u}(\mathbf{x}) = \left[u(x_0)\,, u(x(1))\,, \dots\,, u(x(N-1))\right]$ during the N-step trajectory. The controller performance is quantified by the following cost function over the N-step trajectory

$$V_N(\mathbf{x}(x_0), \mathbf{u}(\mathbf{x})) = \sum_{i=0}^{N-1} l(x_i, u_i)\,. \tag{80}$$

We can then define the convex sublevel set of the cost function as

$$\mathbb{V}(\zeta) = \{x_0 | V_N(\mathbf{x}(x_0), \mathbf{u}(\mathbf{x})) \leq \zeta, \zeta > 0, x_0 \in \mathbb{X}\}\,. \tag{81}$$

The exact computation of the sublevel sets is intractable, due to $\mathbb{X}$ and $\mathbb{U}$ being continuous. Therefore, we use the discretized state space $\mathbb{X}_\delta$ to approximate the sublevel sets of the cost function from simulation by defining the following convex hull

$$\mathbb{V}_\delta(\zeta) = \text{conv}(\{x_0 | V_N(\mathbf{x}(x_0), \mathbf{u}(\mathbf{x})) \leq \zeta, \zeta > 0, x_0 \in \mathbb{X}_\delta\}). \tag{82}$$

The sublevel sets of the cost function are convex sets, consequently, the approximated sublevel sets are inner approximations of the true sublevel set such that

$$\mathbb{V}_\delta(\zeta) \subset \mathbb{V}(\zeta)\,. \tag{83}$$

Smaller discretizations result in a more accurate approximation of the sublevel set $\mathbb{V}(\zeta) = \lim_{\delta \to 0} \mathbb{V}_\delta(\zeta)$. We approximate the sublevel sets $\mathbb{V}_\delta(\zeta)$ using $\mathbb{X}_\delta$ with $\delta = 0.05$ for the sublevels $\zeta \in \{10, 20, ..., 60\}$.

For a given sublevel ζ, the sublevel set of controller A, $\mathbb{V}_A(\zeta)$, may be a subset of the sublevel set of controller B, $\mathbb{V}_B(\zeta)$, which we refer to as 'subset relationship', i.e. $\mathbb{V}_A(\zeta) \subset \mathbb{V}_B(\zeta)$. This indicates that controller B has a higher performance since it stabilizes more states with a cost ζ or lower. Therefore, we determine that a controller is high performance if it has a larger area for a given sublevel set. Note that sublevel sets for a certain controller are not necessarily sub- or supersets of other controllers, we refer to this as 'not a subset relationship'. If two sublevel sets have a 'not a subset relationship', we still compare their areas but cannot conclude that one of the controllers achieves a higher performance for some of the initial states.

7.3 | Accuracy

The controllers aim to drive the system to the origin. We determine the accuracy of a controller by calculating the 2-norm of the final state achieved $x(N)$. We define a controller as accurate if for all feasible states, the 2-norm of the final states are small.

8 | RESULTS

In this section we present the results obtained when applying the evaluation framework detailed in section 7 to the numerical example introduced in section 6. In section 8.1 we compare and validate the estimation of W_{ℓ_1} for the RMPC-ℓ_1 approach and W for the RMPC approach through simulations. Additionally, we present the results for the evaluation framework: *(i)* feasibility in section 8.2, *(ii)* performance measured by the cost in section 8.3, and *(iii)* accuracy of a stabilization task in section 8.4.

8.1 | Validation of Disturbance Sets

In the following, we experimentally validate the robust controllable sets computed in section 7.1. In this section we use the subindex (a, b) for the set of discrete feasible initial states $\mathbb{X}_{(a,b),\delta}$ to denote a simulation horizon a and an optimization horizon b. In order to validate the computed robust controllable sets we compare them with the set of discrete feasible initial states for RMPC and RMPC-ℓ_1 obtained through simulations. We determine the sets of discrete feasible initial states $\mathbb{X}_{(N,H),\delta}$ for RMPC and $\mathbb{X}_{(N,H),\delta,\ell_1}$ for RMPC-ℓ_1 with $\delta = 0.05$. If the disturbance sets W and W_{ℓ_1} are appropriately chosen, then the set of discrete feasible initial states will lie inside the computed robust controllable sets. For this numerical example, we show that $\mathbb{X}_{(N,H),\delta} \subset \mathbb{K}_H(\bar{\mathbb{X}}_f, Z)$ for RMPC and $\mathbb{X}_{(N,H),\delta,\ell_1} \subset \mathbb{K}_{H,\ell_1}(\bar{\mathbb{X}}_{f,\ell_1}, Z_{\ell_1})$ for RMPC-ℓ_1. Furthermore, we show that there are no feasible states outside the computed H-step robust controllable sets. In Fig. 4 the set of discrete feasible initial states $\mathbb{X}_{(N,H),\delta,\ell_1}$ is displayed in green for $\delta = 0.1$ alongside the computed robust controllable set $\mathbb{K}_{H,\ell_1}(\bar{\mathbb{X}}_{f,\ell_1}, Z_{\ell_1})$ for RMPC-ℓ_1 in red. The larger δ was chosen for improved visibility; however, the results hold for $\delta = 0.05$. Similarly, we confirm that the set of discrete feasible initial states $\mathbb{X}_{(N,H),\delta}$ for RMPC lies in the computed H-step robust controllable set for RMPC (not displayed). This validates our choices of W and W_{ℓ_1} for the RMPC and RMPC-ℓ_1.

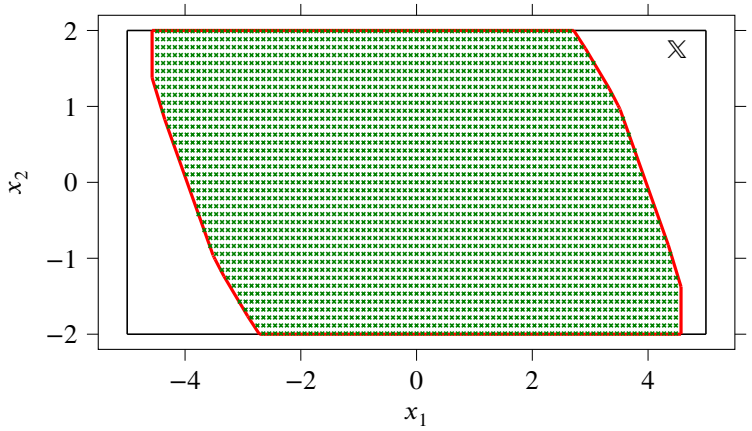

FIGURE 4 H-step robust controllable set $\mathbb{K}_{H,\ell_1}(\bar{\mathbb{X}}_{f,\ell_1}, Z)$ for RMPC-ℓ_1 calculated according to (77) and (78) is shown in red and the feasible discrete initial states $\mathbb{X}_{(N,H),\delta,\ell_1}$ for the proposed RMPC-ℓ_1 obtained from simulation are shown as green crosses with a discretization $\delta = 0.1$. All feasible discrete initial conditions lie exclusively inside the computed H-step robust controllable set, which validates our choice of disturbance set W_{ℓ_1}.

8.2 | Feasibility

In this section we discuss the feasibility of the different controllers as described in section 7.1. A comparison of the controllable sets for the different controllers is shown in Fig. 5. The controllable sets for the controllers without an underlying ℓ_1 AC are a subset of the controllable sets for the same controller with an underlying ℓ_1 AC. The LQR is not able to guarantee feasibility inside its control invariant set $\mathbb{X}_f$ (not displayed here), while the LQR-ℓ_1 is able to successfully control the system inside and a bit beyond its control invariant set $\mathbb{X}_{f,\ell_1}$ (not displayed here). The sets for the MPC and MPC-ℓ_1 do not extend symmetrically along the two dimensions, as it is the case for the LQR, LQR-ℓ_1, RMPC, and RMPC-ℓ_1. The difference in size between the controllable sets of optimization-based controllers with and without ℓ_1 AC is smallest for RMPC and RMPC-ℓ_1. Moreover, it is important to note that neither ℓ_1 AC nor RMPC-ℓ_1 are a subset of the other and their intersection is non-empty. Additionally, the RMPC-ℓ_1 robust controllable set has the largest area of all the compared controllers. The percentages of the relative area

shown in Fig. 5 show that an underlying $\mathscr{L}_1$ AC is able to increase the area of the controllable set for LQR and MPC by 36.46% and 13.70%, respectively. For the RMPC the underlying $\mathscr{L}_1$ AC increases the area of the controllable set by 2.38%. Finally, the combination of an $\mathscr{L}_1$ AC with RMPC increases the area of the controllable set of the $\mathscr{L}_1$ AC by 0.23%, which is the smallest gain in area for the controllable set compared to the other combinations.

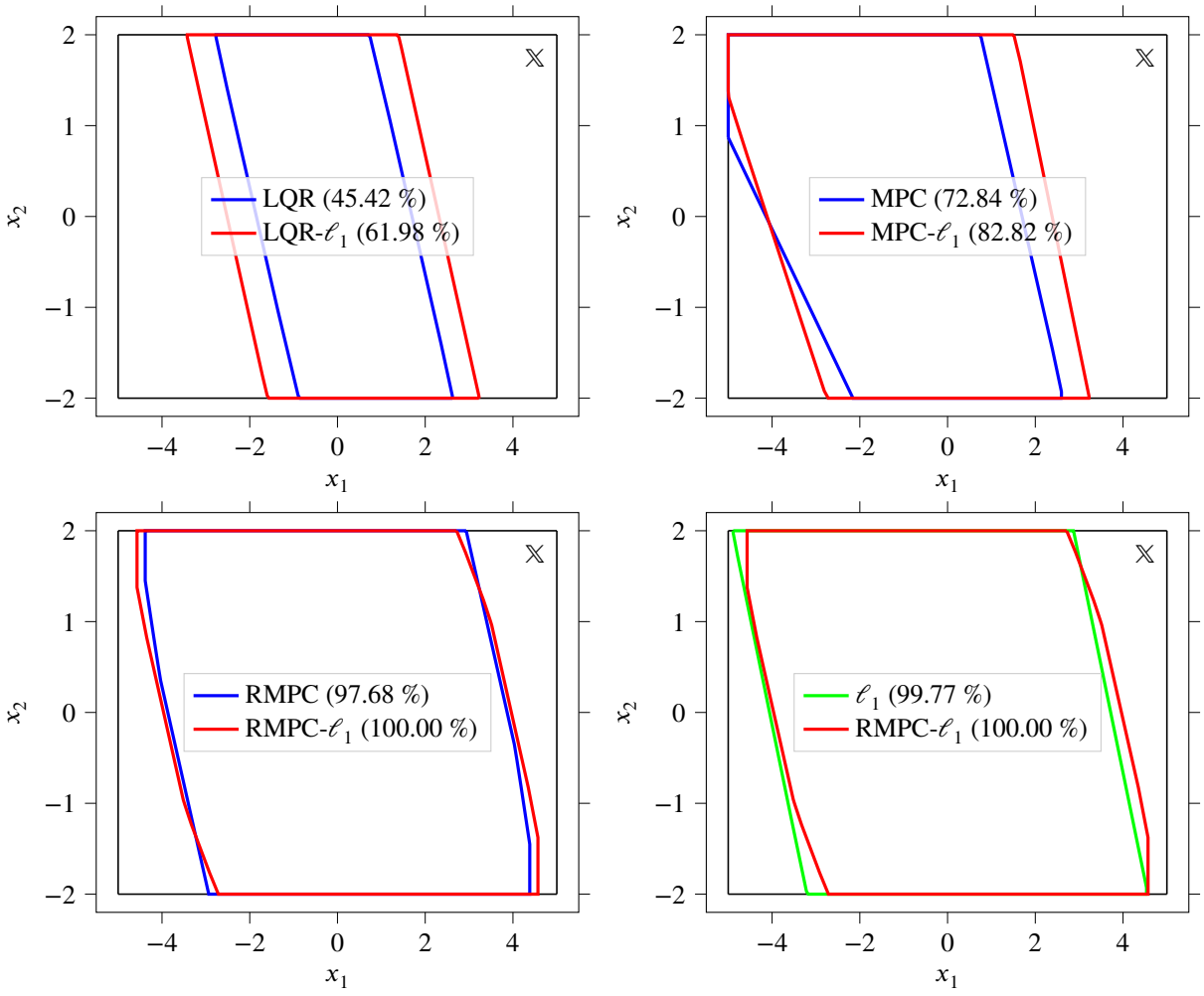

FIGURE 5 Comparison of the controllable sets for the different controllers. The relative area of the controllable set compared to the area of the H-step robust controllable set for the proposed RMPC-$\mathscr{L}_1$ is displayed in parentheses. We show the approximated controllable sets for LQR, LQR-$\mathscr{L}_1$, MPC, MPC-$\mathscr{L}_1$ and the computed H-step robust controllable sets using (77) and (78) for the RMPC and the proposed RMPC-$\mathscr{L}_1$. An underlying $\mathscr{L}_1$ adaptive controller increases the size of the controllable sets. The proposed RMPC-$\mathscr{L}_1$ has the largest controllable set and yields the most feasible initial states.

8.3 | Performance

Our findings regarding the performance of the different controllers as described in section 7.2 are presented in this section. The sublevel sets of the cost function for the $\mathscr{L}_1$ AC and the proposed RMPC-$\mathscr{L}_1$ are displayed in Fig. 6 for the sublevels $\zeta \in \{10, 20, ..., 60\}$. Notice that starting from the origin, the cost increases towards the boundaries of the controllable sets. Furthermore, comparing the sublevel sets for both controllers, it is evident that the sublevel sets for the $\mathscr{L}_1$ AC are subsets of the sublevel sets for the RMPC-$\mathscr{L}_1$ for $\zeta \in \{10, 20, 30\}$. This means that the cost achieved with the RMPC-$\mathscr{L}_1$ is lower than the one obtained with the $\mathscr{L}_1$ AC inside the sublevel set $\mathbb{V}_{\text{RMPC}-\mathscr{L}_1}(\zeta = 30)$.

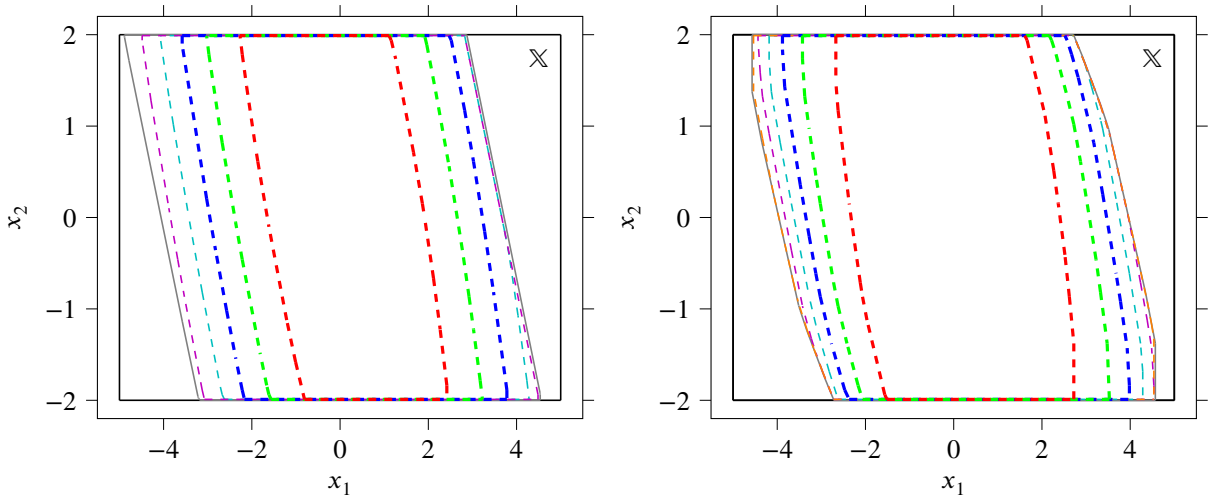

(a) Cost sublevel sets for ℓ_1 AC.

(b) Cost sublevel sets for the proposed RMPC-ℓ_1.

FIGURE 6 Comparison of the approximated cost sublevel sets for ℓ_1 AC and the proposed RMPC-ℓ_1. The sublevel sets are shown for $\zeta \in \{10, 20, ..., 60\}$, where the innermost set (dashed red line) represents the sublevel with $\zeta = 10$ and the outermost set (dashed purple line for the ℓ_1 and dashed orange line for the RMPC-ℓ_1) represents $\zeta = 50$ for the ℓ_1 AC and $\zeta = 60$ for the RMPC-ℓ_1. The sublevel sets for $\zeta \in \{10, 20, 30\}$ for the ℓ_1 AC are subsets of the corresponding sublevel sets for the proposed RMPC-ℓ_1, which indicates a better performance for the proposed RMPC-ℓ_1 for those levels.

The areas of the sublevel sets of the cost function for the baseline controllers are compared to the corresponding sublevel sets for the RMPC-ℓ_1 controller. A summary of these comparisons is found in Tab. 1. Note that the maximum cost achieved for LQR, LQR-ℓ_1, RMPC and ℓ_1 AC is less than the sublevel set value $V_{N,\max} = \max_{x_0} V_N(\mathbf{x}(x_0), \mathbf{u}(\mathbf{x})) \leq \zeta$ for sublevel $\zeta = 20, 20, 60, 60$, respectively. For these controllers, all subsequent sublevel sets are equal to the controllable set $\mathbb{V}_\delta(\zeta) = \mathbb{K}_{N,\delta}, \forall \zeta \geq V_{N,\max}$. The sublevels at which the sublevel sets of the baseline controllers have a 'not a subset' relationship with the corresponding sublevel sets of the proposed controller are shown in brackets in Tab. 1. Note that LQR and LQR-ℓ_1 switch from having a 'not a subset' relationship with the proposed RMPC-ℓ_1 to a subset relationship at sublevel $\zeta = 20$, respectively. On the other hand, ℓ_1 AC switches from a subset relationship to 'not a subset' relationship at $\zeta = 40$. Additionally, there is no ζ for which MPC, MPC-ℓ_1, and RMPC have a subset relationship with RMPC-ℓ_1.

From Tab. 1, the ℓ_1 AC has the smallest sublevel set for the sublevel $\zeta = 10$, which implies that only a small portion of the feasible initial states incurrs in such a small cost. In most cases, an underlying ℓ_1 AC is able to increase the area of the sublevel sets compared to the same controller without an underlying ℓ_1 AC. The only exceptions is for the cost level $\zeta = 10$ for the RMPC and RMPC-ℓ_1. This is one of the two sublevels where the proposed RMPC-ℓ_1 does not have the greatest area for the corresponding sublevel sets. This is due to two main causes *(i)* RMPC has a more aggressive response than RMPC-ℓ_1 due to ℓ_1 initializing with the wrong estimates for the parameters, and *(ii)* the disturbance (and the resulting modeling error) is smaller for smaller states. Similar effects cause MPC-ℓ_1 to have a slightly larger area than RMPC-ℓ_1 for sublevel $\zeta = 10$.

With increasing ζ, the area of the sublevel sets from ℓ_1 AC get closer to the ones from RMPC-ℓ_1 until the area of its sublevel set at $\zeta = 60$ is marginally greater. The sublevel sets for RMPC have a similar area compared to those for RMPC-ℓ_1. MPC and MPC-ℓ_1 are the only controllers, besides RMPC-ℓ_1, that reach the maximum cost $V_{N,\max} \geq 60$. Finally, the sublevel sets of the RMPC-ℓ_1 have a greater area than the sublevel sets of the ℓ_1 AC throughout the different sublevels ζ, except $\zeta = 60$, which indicates that the cost achieved by RMPC-ℓ_1 until $\zeta = 60$ is lower than the cost obtained by ℓ_1 AC for a larger set of initial states.

8.4 | Accuracy

In this section we evaluate the accuracy of the different controllers as described in section 7.3. We begin by comparing the accuracy of RMPC, ℓ_1 AC, and RMPC-ℓ_1 for the same initial state. Finally, we analyze the accuracy by comparing the steady-state error for all feasible discrete initial states for all controllers.

TABLE 1 Performance cost function sublevel set areas in the state space for baseline controllers as a percentage relative to the proposed RMPC-ℓ_1 sublevel set areas for different sublevels ζ. Gray denotes that the maximum cost obtained by the controller is less than ζ, such that all subsequent sublevel sets are equal to the controllable set. $[\cdot]$ indicates that neither of the sublevel sets is a subset of the other. Green highlights the smaller sublevel set areas for the ℓ_1 AC, indicating a higher cost for the ℓ_1 AC. Blue highlights sublevel sets with greater area than the corresponding sublevel set for the RMPC-ℓ_1. The difference is marginal, therefore, an underlying ℓ_1 AC does not degrade performance for the RMPC-ℓ_1.

ζ	LQR [%]	LQR-ℓ_1 [%]	MPC [%]	MPC-ℓ_1 [%]	RMPC [%]	ℓ_1 AC [%]	RMPC-ℓ_1 [%]
10	[77.10]	[98.00]	[87.96]	[100.88]	[100.49]	75.53	100.00
20	59.91	81.76	[80.15]	[91.77]	[99.97]	84.04	100.00
30	52.95	72.25	[76.20]	[87.92]	[99.67]	91.23	100.00
40	48.90	66.73	[73.29]	[84.59]	[99.19]	[96.62]	100.00
50	46.57	63.55	[71.62]	[82.33]	[98.27]	[98.08]	100.00
60	45.77	62.46	[71.44]	[81.66]	[98.44]	[100.52]	100.00

We compare the accuracy of RMPC, ℓ_1 AC, and the proposed RMPC-ℓ_1 using the initial state $x_0 = [\,-3.0 \quad -1.0\,]^T$, which is feasible for all three controllers. In Fig. 7 we present a detailed trajectory and the corresponding sets for the proposed RMPC-ℓ_1. The RMPC-ℓ_1 drives the system towards the origin, while the calculated optimal state sequence $\mathbf{x}^*_{\text{RMPC}-\ell_1}(x_0) = [\,x_0^*(x_0), x_0^*(x(1)), \ldots, x_0^*(x(N))\,]$ stays inside the tightened constrained set $\bar{\mathbb{X}}_{\ell_1}$ and the trajectory of visited states $\mathbf{x}_{\text{RMPC}-\ell_1}(x_0)$ does not leave the constrained set $\mathbb{X}$. The right side of Fig. 7 shows a detail of the trajectory around the origin. The trajectory taken by the RMPC-ℓ_1 is able to steer the system to the origin in N steps.

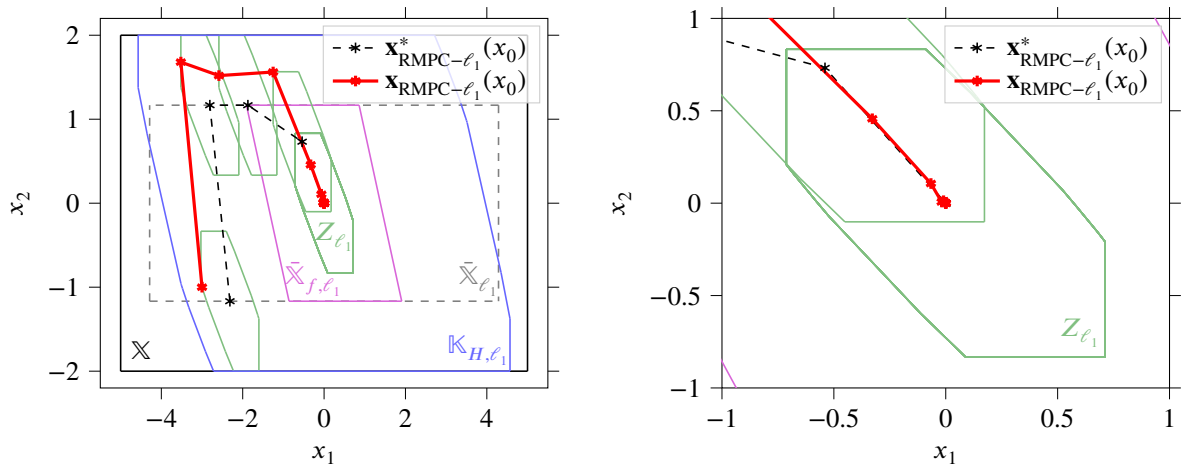

FIGURE 7 Feasible trajectory for the initial condition $x_0 = [\,-3.0 \quad -1.0\,]^T$ controlled by the proposed RMPC-ℓ_1. The left plots shows the full state trajectory in red and the calculated optimal state sequence in black dashed lines. Also shown are the tightened terminal $\bar{\mathbb{X}}_{f,\ell_1}$, tightened state constraint $\bar{\mathbb{X}}_{\ell_1}$, state constraint $\mathbb{X}_{\ell_1}$ and robust controllable $\mathbb{K}_{H,\ell_1}$ sets. The plot on the right shows that the RMPC-ℓ_1 successfully steers the system to the origin in N steps, while all state and input constraints are satisfied for every time step.

In Fig. 8 we compare the resulting trajectories for the same initial condition $x_0 = [\,-3.0 \quad -1.0\,]^T$ for the RMPC, ℓ_1 AC, and the proposed RMPC-ℓ_1. All controllers are able to control the system without violating any constraints, even though they are not explicitly enforced for the ℓ_1 AC. A detail of the trajectory around the origin is depicted on the right side of Fig. 8. The system controlled by the RMPC does not reach the origin and oscillates, but stays inside its disturbance invariant set Z (not shown here). From the detail on the right plot, it is evident that the ℓ_1 AC controlled system has not reached its steady-state

after N steps and requires more steps to reach the origin. For this initial condition the proposed RMPC-$\mathscr{E}_1$ is the only controller which steers the system to the origin in N steps.

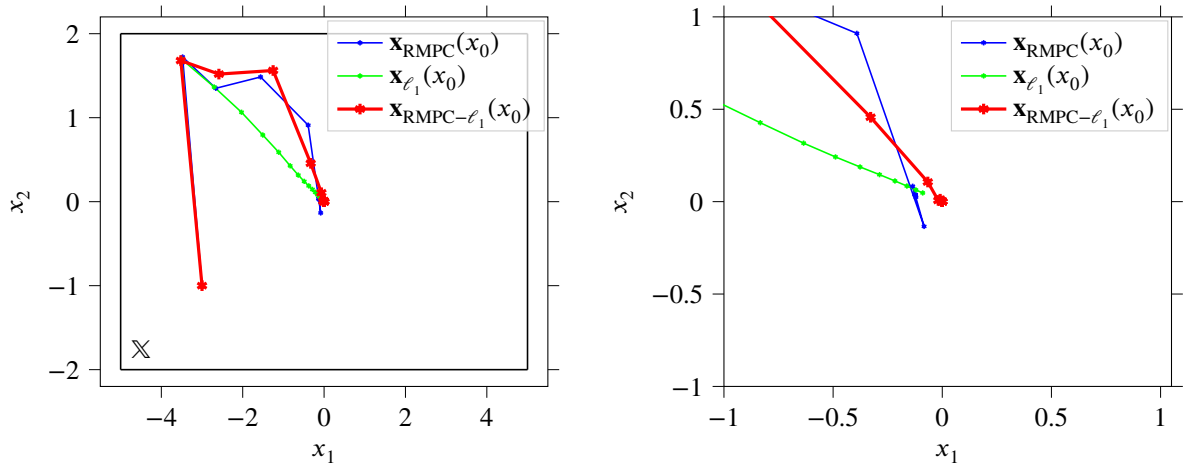

FIGURE 8 Comparison of feasible trajectories from the initial condition $x_0 = [\,-3.0 \quad -1.0\,]^T$ for the system controlled by the RMPC, $\mathscr{E}_1$ AC, and the proposed RMPC-$\mathscr{E}_1$. While neither the RMPC, nor the $\mathscr{E}_1$ AC are able to control the system to the origin, the system controlled by the proposed RMPC-$\mathscr{E}_1$ successfully reaches the origin in N steps.

For the accuracy analysis over the state space we use the feasible initial states from the discretized feasible state space $\mathbb{X}_{H,\,\delta}$ for the proposed RMPC-$\mathscr{E}_1$ and each of the baseline controllers. For each feasible initial state of each controller, we determine the final state $x(N)$ in simulation and show in Tab. 2 the minimum and maximum errors of the final states, measured as described in section 7.3. From Tab. 2 it is evident that LQR, MPC, and RMPC have an error $\Delta x = 0.12423$. By using an underlying $\mathscr{E}_1$ AC, the maximum and minimum errors of LQR, MPC and RMPC decrease by factors greater than 12000. The maximum and minimum errors of each controller are almost identical for all the controllers except $\mathscr{E}_1$ AC. This indicates that the error for these controllers does not depend on the initial condition. The $\mathscr{E}_1$ AC achieves a minimum error closer in magnitude to those achieved by LQR, MPC and RMPC with underlying $\mathscr{E}_1$ AC, but a maximum error close to the error achieved by LQR, MPC, and RMPC. Therefore, the error from the $\mathscr{E}_1$ AC depends on the initial condition. This is related to what is observed in Fig. 8 where N steps are not sufficient for the $\mathscr{E}_1$ AC to converge to the origin for all feasible initial conditions. The errors obtained by the LQR-$\mathscr{E}_1$, the MPC-$\mathscr{E}_1$, and the RMPC-$\mathscr{E}_1$ can be regarded as negligible.

TABLE 2 For all feasible initial states in the discretized state space, for all the controllers, we show the maximum and minimum errors incurred at the final state $x(N)$. The accuracy of the optimization-based controllers is significantly improved by combining them with an underlying $\mathscr{E}_1$ AC. Similarly, the accuracy of the $\mathscr{E}_1$ AC is significantly improved by combining it with an optimization-based controller.

Error	$\mathscr{E}_1$ AC	LQR	LQR-$\mathscr{E}_1$	MPC	MPC-$\mathscr{E}_1$	RMPC	RMPC-$\mathscr{E}_1$
$\Delta x_{\text{min},\,N}$	< 0.00001	0.12423	< 0.00001	0.12423	< 0.00001	0.12423	< 0.00001
$\Delta x_{\text{max},\,N}$	0.08785	0.12423	< 0.00001	0.12423	< 0.00001	0.12423	< 0.00001

9 | DISCUSSION

In this section we evaluate the feasibility, performance, and accuracy of the proposed RMPC-$\mathscr{L}_1$ controller as compared to the baseline controllers. Our experimental results lead us to the following three main conclusions: *(i)* the $\mathscr{L}_1$ AC increases the feasibility of the optimization-based controllers with RMPC-$\mathscr{L}_1$ achieving the largest robust controllable set; *(ii)* combining $\mathscr{L}_1$ AC with RMPC does not negatively affect the performance of the RMPC; and *(iii)* combining $\mathscr{L}_1$ adaptive control with optimization-based controllers significantly improves the accuracy of the optimization-based controllers.

The feasibility analysis highlights that an underlying $\mathscr{L}_1$ AC increases the size of the controllable sets for all examined optimization-based controllers. The controllable sets for LQR-$\mathscr{L}_1$ and MPC-$\mathscr{L}_1$ are smaller than the controllable set of $\mathscr{L}_1$ AC, while the controllable set for RMPC-$\mathscr{L}_1$ is larger than the controllable set for $\mathscr{L}_1$ AC alone. We emphasize that we compare the robust controllable sets for RMPC and RMPC-$\mathscr{L}_1$, computed using (77) and (78), to outer approximations of the controllable sets for the other controllers, obtained through simulation. Therefore, the true difference between the size of the robust controllable and controllable sets is even larger. The $\mathscr{L}_1$ AC yields the second largest controllable set, but does not allow the calculation of its controllable set *a priori*. Furthermore, the approximated controllable set is only valid for specific uncertainties θ and ξ, whereas the robust controllable sets for RMPC and RMPC-$\mathscr{L}_1$ are valid for all possible uncertainties that lie within the parameter sets Θ and Ξ, specified in Assumption 1. The robust controllable set for RMPC-$\mathscr{L}_1$ is valid even at the beginning of the simulation when the $\mathscr{L}_1$ AC has large parameter uncertainties, since the parameter estimates are guaranteed to be contained in Θ and Ξ. In practice, an *a priori* unknown controllable set could result in a failure when applying the $\mathscr{L}_1$ AC at infeasible initial conditions.

The performance evaluation of all the controllers suggests that overall RMPC and RMPC-$\mathscr{L}_1$ obtain the lowest costs for the tested feasible initial conditions. The sublevel sets for low values of ζ have a small area in the state space for the $\mathscr{L}_1$ AC, because the desired objective is unknown to the $\mathscr{L}_1$ AC. Combining the $\mathscr{L}_1$ AC with RMPC enables the implementation of a performance objective for the $\mathscr{L}_1$ adaptive controller. Moreover, the results presented in section 8 demonstrate that RMPC-$\mathscr{L}_1$ has a marginally worse performance for the first sublevel $\zeta = 10$ than RMPC and MPC-$\mathscr{L}_1$. However, the proposed RMPC-$\mathscr{L}_1$ outperforms all baseline controllers for all subsequent sublevels $\zeta \in \{20, 30, 40, 50\}$, i.e. when the underlying $\mathscr{L}_1$ AC is better able to cancel the uncertainties in the system. At $\zeta = 60$ the $\mathscr{L}_1$ AC only marginally outperforms the RMPC-$\mathscr{L}_1$.

By comparing the trajectories that the proposed and baseline controllers follow for the same initial states, we are able to demonstrate the ability of the RMPC-$\mathscr{L}_1$ to control the disturbed system to the origin in a limited number of time steps N. In particular, the system controlled by the RMPC oscillates between states located close to the origin, while the system controlled by $\mathscr{L}_1$ AC has not reached its steady-state after N time steps. The improved accuracy of the proposed RMPC-$\mathscr{L}_1$ is achieved by leveraging two characteristics of the proposed controller: *(i)* using the adaptation and control laws, the $\mathscr{L}_1$ adaptive controller helps to cancel the uncertainties in the system and makes the system behave close to the nominal model; and *(ii)* the RMPC uses this nominal model to optimize the performance of the system. Notice that the RMPC is not able to follow its predicted state trajectory to the origin due to the existing model mismatch. However, the proposed RMPC-$\mathscr{L}_1$ is able to reach the origin as predicted since the uncertainties are handled by the $\mathscr{L}_1$ adaptive controller. We also compare the accuracy of all feasible discrete initial states for all controllers, and show that combining $\mathscr{L}_1$ adaptive controller with the optimization-based controllers significantly improves their accuracy since the model uncertainties are handled by the $\mathscr{L}_1$ adaptive controller.

The proposed RMPC-$\mathscr{L}_1$ combines the advantages of the $\mathscr{L}_1$ AC and the RMPC. The RMPC component guarantees constraint satisfaction for initial conditions inside the H-step robust controllable set for all possible model mismatch and for an $\mathscr{L}_1$ AC that initially has large parameter estimation inaccuracies. Moreover, it allows the specification of a user-defined objective with a cost function. This enables more aggressive control inputs, which leads to the stabilization at the origin in only N time steps. The underlying $\mathscr{L}_1$ AC contributes by improving the disturbance cancellation at every time step, which enables accurate stabilization to the origin. Finally, the underlying $\mathscr{L}_1$ AC does not degrade the high-level RMPC performance.

10 | CONCLUSION

In this paper we introduced a novel robust adaptive MPC framework to guarantee fast and accurate stabilization in the presence of modeling errors, while guaranteeing feasibility for as many different initial conditions as possible. The proposed RMPC-$\mathscr{L}_1$ consists of an underlying discrete-time state feedback $\mathscr{L}_1$ adaptive controller and a robust MPC. In this work we: *(i)* introduce a modified discrete-time state feedback $\mathscr{L}_1$ adaptive controller; *(ii)* provide its stability and performance proofs; *(iii)* use the performance proofs in a robust MPC framework; and *(iv)* validate the feasibility, performance, and accuracy of the proposed

RMPC-ℓ_1 on a stabilization task. Ideally, the discrete-time state feedback ℓ_1 adaptive controller makes the system behave as a linear reference model. In reality, the behavior of the real system may deviate from the linear reference model. In this work, we show that this deviation is uniformly bounded and can be thought of as the modeling error. A robust MPC is then used to compute an optimal input, which serves as a reference to the ℓ_1 AC while taking into account the modeling error. On the stabilization task we demonstrate that the proposed RMPC-ℓ_1 yields constraint satisfaction for the most initial states compared to other baseline controllers. Given a performance objective, the RMPC-ℓ_1 achieves a performance similar or better than the other baseline controllers. Finally, the RMPC-ℓ_1 is able to accurately control the system to the origin with no offset in a limited number of time steps.

How to cite this article: Pereida K., Brunke L. and Schoellig A. P. (2021), Robust adaptive model predictive control for guaranteed fast and accurate stabilization in the presence of model errors, *Int J Robust Nonlinear Control.*, *2021;1–35. https://doi.org/10.1002/rnc.5712*.

APPENDIX

A SUPPLEMENTAL MATERIALS

A.1 Proof of Lemma 1

The proof of Lemma 1 is presented next.

Proof. Define

$$F \triangleq \tfrac{1}{\sigma} P^{\frac{1}{2}} A_m\,,\; G \triangleq \sigma P^{\frac{1}{2}} b_m\,,\; J(\tilde{x}(k)) \triangleq \tilde{x}^T(k) P \tilde{x}(k)\,. \tag{A1}$$

Then,

$$\begin{aligned}
\Delta J_{\tilde{x}}(k) &\triangleq \tilde{x}^T(k+1)P\tilde{x}(k+1) - \tilde{x}^T(k)P\tilde{x}(k)\\
&= (A_m\tilde{x}(k) + b_m(\tilde{\theta}^T(k)x(k) + \tilde{\xi}(k)))^T P(A_m\tilde{x}(k) + b_m(\tilde{\theta}^T(k)x(k) + \tilde{\xi}(k))) - \tilde{x}^T(k)P\tilde{x}(k)\\
&= \tilde{x}^T(k)A_m^T P A_m\tilde{x}(k) + \tilde{x}^T(k)A_m^T P b_m(\tilde{\theta}^T(k)x(k) + \tilde{\xi}(k)) + (x^T(k)\tilde{\theta}(k) + \tilde{\xi}(k))b_m^T P A_m\tilde{x}(k)\\
&\quad +(x^T(k)\tilde{\theta}(k) + \tilde{\xi}(k))b_m^T P b_m(\tilde{\theta}^T(k)x(k) + \tilde{\xi}(k)) - \tilde{x}^T(k)P\tilde{x}(k)\\
&= \tilde{x}^T(k)(A_m^T P A_m - P)\tilde{x}(k) + \tilde{x}^T(k)A_m^T P b_m(x^T(k)\tilde{\theta}(k) + \tilde{\xi}(k))\\
&\quad +(x^T(k)\tilde{\theta}(k) + \tilde{\xi}(k))b_m^T P A_m\tilde{x}(k) + (x^T(k)\tilde{\theta}(k) + \tilde{\xi}(k))^2 b_m^T P b_m\\
&= \tilde{x}^T(k)(A_m^T P A_m - P + F^T F)\tilde{x}(k) - \tilde{x}^T(k)F^T F\tilde{x}(k) + \tilde{x}^T(k)F^T G(x^T(k)\tilde{\theta}(k) + \tilde{\xi}(k))\\
&\quad +(x^T(k)\tilde{\theta}(k) + \tilde{\xi}(k))G^T F\tilde{x}(k) + (x^T(k)\tilde{\theta}(k) + \tilde{\xi}(k))^2 b_m^T P b_m + (\tilde{x}^T(k)\tilde{\theta}(k) + \tilde{\xi}(k))^2 G^T G\\
&\quad -(\tilde{x}^T(k)\tilde{\theta}(k) + \tilde{\xi}(k))^2 G^T G\\
&= \tilde{x}^T(k)(A_m^T P A_m - P + F^T F)\tilde{x}(k) + (x^T(k)\tilde{\theta}(k) + \tilde{\xi}(k))^2(b_m^T P b_m + G^T G)\\
&\quad - \begin{bmatrix}\tilde{x}^T(k) & -(x^T(k)\tilde{\theta}(k) + \tilde{\xi}(k))\end{bmatrix}\begin{bmatrix}F^T F & F^T G\\ G^T F & G^T G\end{bmatrix}\begin{bmatrix}\tilde{x}(k)\\ -(x^T(k)\tilde{\theta}(k) + \tilde{\xi}(k))\end{bmatrix}\\
&\leq \tilde{x}^T(k)(A_m^T P A_m - P + F^T F)\tilde{x}(k) + (x^T(k)\tilde{\theta}(k) + \tilde{\xi}(k))^2(b_m^T P b_m + G^T G)\,.
\end{aligned} \tag{A2}$$

The last inequality is possible since the symmetric product of F, G is positive semidefinitive. Note that

$$F^T F = \frac{1}{\sigma^2} A_m^T P A_m = \frac{A_m^T P A_m}{\lambda_{\max}(A_m^T P A_m)} \preccurlyeq \frac{I_n \lambda_{\max}(A_m^T P A_m)}{\lambda_{\max}(A_m^T P A_m)} = I_n\,. \tag{A3}$$

It follows from (13) that

$$A_m^T P A_m - P + F^T F \preccurlyeq A_m^T P A_m - P + I_n = -R\,. \tag{A4}$$

Therefore,

$$\tilde{x}^T(k)(A_m^T P A_m - P + F^T F)\tilde{x}(k) \leq -\tilde{x}^T(k)R\tilde{x}(k)\,, \tag{A5}$$

which implies

$$\Delta J_{\tilde{x}}(k) \leq -\tilde{x}^T(k)R\tilde{x}(k) + (x^T(k)\tilde{\theta}(k) + \tilde{\xi}(k))^2(b_m^T P b_m + G^T G)\,, \quad G^T G = \sigma^2 b_m^T P b_m\,, \tag{A6}$$

then

$$\Delta J_{\tilde{x}}(k) \leq -\tilde{x}^T(k)R\tilde{x}(k) + (x^T(k)\tilde{\theta}(k) + \tilde{\xi}(k))^2((1+\sigma^2) b_m^T P b_m)\,. \tag{A7}$$

Since $\ln x \leq x - 1$ for all $x \geq 0$,

$$\begin{aligned}\Delta V_x(\tilde{x}(k)) &= \ln(1 + \mu\tilde{x}^T(k+1)P\tilde{x}(k+1)) - \ln(1 + \mu\tilde{x}^T(k)P\tilde{x}(k)) \\ &= \ln\left(\frac{1 + \mu\tilde{x}^T(k+1)P\tilde{x}(k+1)}{1 + \mu\tilde{x}^T(k)P\tilde{x}(k)}\right) = \ln\left(1 + \frac{\mu\Delta J_{\tilde{x}}(k)}{1 + \mu\tilde{x}^T(k)P\tilde{x}(k)}\right) \\ &\leq \frac{\mu\Delta J_{\tilde{x}}(k)}{1 + \mu\tilde{x}^T(k)P\tilde{x}(k)} \leq \mu\frac{[-\tilde{x}^T(k)R\tilde{x}(k) + (x^T(k)\tilde{\theta}(k) + \tilde{\xi}(k))^2((\sigma^2+1)b_m^T P b_m)]}{1 + \mu\tilde{x}^T(k)P\tilde{x}(k)}.\end{aligned} \tag{A8}$$

□

A.2 Proof of Lemma 2

The proof of Lemma 2 is presented next.

Proof. Using the z-transform and (8), we can write (16) as

$$\hat{x}(z) = G(z)\hat{\eta}(z) + k_g H(z)C(z)r(z) + x_{in}(z), \tag{A9}$$

where $x_{in}(z)$ captures the initial conditions and is defined in (15) and $G(z)$, $H(z)$ were defined as in (10). For all $k \in \{0, \dots, k' - 1\}$, the following bounds hold:

$$\begin{aligned}\|\hat{x}|_k\|_{\ell_\infty} &\leq \|G(z)\|_{\ell_1}\|\hat{\eta}|_k\|_{\ell_\infty} + \|k_g H(z)C(z)\|_{\ell_1}\|r|_k\|_{\ell_\infty} + \|x_{in}|_k\|_{\ell_\infty} \\ \|\hat{\eta}|_k\|_{\ell_\infty} &\leq L_\theta\left(\|\tilde{x}|_k\|_{\ell_\infty} + \|\hat{x}|_k\|_{\ell_\infty}\right) + L_\xi.\end{aligned} \tag{A10}$$

Using the definition of λ_θ in (9), we can write the above inequalities as:

$$\|\hat{x}|_k\|_{\ell_\infty} \leq \frac{1}{1 - \lambda_\theta}\left(\lambda_\theta\|\tilde{x}|_k\|_{\ell_\infty} + \|G(z)\|_{\ell_1}L_\xi + \|k_g H(z)C(z)\|_{\ell_1}\|r|_k\|_{\ell_\infty} + \|x_{in}|_k\|_{\ell_\infty}\right) \tag{A11}$$

The above can be rewritten using the definitions in (14) as:

$$\|\hat{x}|_k\|_{\ell_\infty} \leq c_1\|\tilde{x}|_k\|_{\ell_\infty} + c_2. \tag{A12}$$

Using the assumption that $\|\tilde{x}|_k\|_{\ell_\infty} \leq \gamma_0$ for $k \in \{0, \dots, k' - 1\}$ for a given k', we can rewrite the above equation as:

$$\|\hat{x}|_k\|_{\ell_\infty} \leq c_1\gamma_0 + c_2. \tag{A13}$$

Then, we obtain a relationship between the squared terms $\|\hat{x}|_k\|^2_{\ell_\infty}$ and $\|\tilde{x}|_k\|^2_{\ell_\infty}$ using the fact that $(c_1\|\tilde{x}|_k\|_{\ell_\infty} - c_2)^2 \geq 0 \iff c_1^2\|\tilde{x}|_k\|^2_{\ell_\infty} + c_2^2 \geq 2c_1c_2\|\tilde{x}|_k\|_{\ell_\infty}$:

$$\|\hat{x}|_k\|^2_{\ell_\infty} \leq 2c_1^2\gamma_0^2 + 2c_2^2. \tag{A14}$$

Recall that n is the state dimension, then the following holds

$$\hat{x}^T(k)\hat{x}(k) \leq n\|\hat{x}|_k\|^2_{\ell_\infty}. \tag{A15}$$

Hence, using (A14), we can write an upper bound for $\hat{x}^T(k)\hat{x}(k)$ as:

$$\hat{x}^T(k)\hat{x}(k) \leq 2nc_1^2\|\tilde{x}|_k\|^2_{\ell_\infty} + 2nc_2^2 \leq 2nc_1^2\gamma_0^2 + 2nc_2^2. \tag{A16}$$

Then, using the definition of $\tilde{x}$ and the fact that $x^T(k)x(k) \geq 0 \iff \hat{x}^T(k)\hat{x}(k) + \tilde{x}^T(k)\tilde{x}(k) \geq 2\hat{x}^T(k)\tilde{x}(k)$, we can get a relationship between $x^T(k)x(k)$ and $\tilde{x}^T(k)\tilde{x}(k)$ as:

$$x^T(k)x(k) \leq 2\hat{x}^T(k)\hat{x}(k) + 2\tilde{x}^T(k)\tilde{x}(k) \leq (4nc_1^2\gamma_0^2 + 4nc_2^2) + 2\tilde{x}^T(k)\tilde{x}(k). \tag{A17}$$

Defining

$$\alpha = 4nc_1^2\gamma_0^2 + 4nc_2^2, \tag{A18}$$

we can show that

$$1 + x^T(k)x(k) \leq 1 + \alpha + 2\tilde{x}^T(k)\tilde{x}(k) = (1 + \alpha)\left(1 + \frac{2\tilde{x}^T(k)\tilde{x}(k)}{1 + \alpha}\right) \leq (1 + \alpha)\left(1 + \mu\tilde{x}^T(k)P\tilde{x}(k)\right), \tag{A19}$$

where

$$\mu = \frac{2}{\lambda_{\min}(P)(1 + \alpha)} > 0, \tag{A20}$$

where $\lambda_{\min}(P)$ is the minimum eigenvalue of P, which completes the proof. □

A.3 Proof of Lemma 3

The proof of Lemma 3 is found next.

Proof. We show this proof by contradiction. Assume that at $k' \in \mathbb{N}$ the inequality $\|\tilde{x}|_{k'}\|_{\ell_\infty} \leq \gamma_0$ is violated for the first time, i.e.,

$$\|\tilde{x}|_k\|_{\ell_\infty} \leq \gamma_0\,, \quad k \in \{0, \dots, k'-1\}\,, \quad \|\tilde{x}|_{k'}\|_{\ell_\infty} > \gamma_0\,. \tag{A21}$$

Recall that $\tilde{x}(0) = 0$. For $k \in \{0, \dots, k'-1\}$, consider the Lyapunov function candidate:

$$V(\tilde{x}(k), \tilde{\rho}(k)) \triangleq V_x(\tilde{x}(k)) + \tau V_\rho(\tilde{\rho}(k))\,, \tag{A22}$$

where

$$V_\rho(\tilde{\rho}(k)) \triangleq \tilde{\rho}^T(k)\tilde{\rho}(k)\,, \tag{A23}$$

$V_x(\tilde{x}(k))$ is defined in (20), and $\tau > 0$ a later specified constant. We also define

$$\Delta V(\tilde{x}(k), \tilde{\rho}(k)) = \Delta V_x(\tilde{x}(k)) + \tau \Delta V_\rho(\tilde{\rho}(k))\,, \tag{A24}$$

where

$$\Delta V_\rho(\tilde{\rho}(k)) = V_\rho(\tilde{\rho}(k+1)) - V_\rho(\tilde{\rho}(k))\,, \tag{A25}$$

and $\Delta V_x(\tilde{x}(k))$ is defined in (21). The orthogonal projection (5) in the adaptation law that keeps the estimate $\hat{\rho}(k)$ in the set $\Theta \times \Xi$ incurs in a lower value of $\Delta V_\rho(\tilde{\rho}'(k+1))$ than when no orthogonal projection is used $\Delta V_\rho(\tilde{\rho}(k+1))$. The latter means that only the upper bound for $\Delta V_\rho(\tilde{\rho}(k+1))$ is needed to draw conclusions for both cases. Note that from (6), we can write:

$$\tilde{\rho}'^T(k+1)\tilde{\rho}'(k+1) \leq \tilde{\rho}^T(k+1)\tilde{\rho}(k+1)\,, \tag{A26}$$

where $\tilde{\rho}'(k+1) = \tilde{\rho}'(k+1) - \rho$. Hence, if the orthogonal projection is used,

$$\Delta V_\rho(\tilde{\rho}'(k)) = \tilde{\rho}'^T(k+1)\tilde{\rho}'(k+1) - \tilde{\rho}^T(k)\tilde{\rho}(k) \leq \tilde{\rho}^T(k+1)\tilde{\rho}(k+1) - \tilde{\rho}^T(k)\tilde{\rho}(k) = \Delta V_\rho(\tilde{\rho}(k))\,. \tag{A27}$$

Since $\Delta V_\rho(\tilde{\rho}'(k)) \leq \Delta V_\rho(\tilde{\rho}(k))$, we will focus the analysis on $\Delta V_\rho(\tilde{\rho}(k))$. From (3) and (4), we can write:

$$\begin{aligned}
\tilde{\rho}(k+1) &= \tilde{\rho}(k) + \frac{\begin{bmatrix} x(k) \\ 1 \end{bmatrix}\left[b_0^T\left(b_m \rho^T \begin{bmatrix} x(k) \\ 1 \end{bmatrix}\right) - \hat{\rho}^T(k)\begin{bmatrix} x(k) \\ 1 \end{bmatrix}\right]}{1 + x^T(k)x(k)} \\
&= \tilde{\rho}(k) + \frac{\begin{bmatrix} x(k) \\ 1 \end{bmatrix}\left[(\rho^T - \hat{\rho}^T(k))\begin{bmatrix} x(k) \\ 1 \end{bmatrix}\right]}{1 + x^T(k)x(k)} = \tilde{\rho}(k) - \frac{\begin{bmatrix} x(k) \\ 1 \end{bmatrix}\tilde{\rho}^T(k)\begin{bmatrix} x(k) \\ 1 \end{bmatrix}}{1 + x^T(k)x(k)} \\
&= \left(\underbrace{I_{n+1} - \frac{\begin{bmatrix} x(k) \\ 1 \end{bmatrix}\begin{bmatrix} x(k) \\ 1 \end{bmatrix}^T}{1 + x^T(k)x(k)}}_{\Phi(x(k))}\right)\tilde{\rho}(k)\,.
\end{aligned} \tag{A28}$$

Note that $\Phi^T(x(k)) = \Phi(x(k)) \geq 0$. Then, $\Delta V_\rho(\tilde{\rho}(k)) = \tilde{\rho}^T(k+1)\tilde{\rho}(k+1) - \tilde{\rho}^T(k)\tilde{\rho}(k) = \tilde{\rho}^T(k)\Phi^T(x(k))\Phi(x(k))\tilde{\rho}(k) - \tilde{\rho}^T(k)\tilde{\rho}(k) = \tilde{\rho}^T(k)(\Phi^T(x(k))\Phi(x(k)) - I_{n+1})\tilde{\rho}(k)$. Also note that $0 \leq \Phi(x(k)) \leq I_{n+1}$ and $\Phi(x(k))\Phi(x(k)) = \Phi(x(k))$. Consequently, $\Phi(x(k))\Phi(x(k)) - I_{n+1} = \Phi(x(k)) - I_{n+1}$ and

$$\Delta V_\rho(\tilde{\rho}(k)) = \tilde{\rho}^T(k)(\Phi(x(k)) - I_{n+1})\tilde{\rho}(k) = -\tilde{\rho}^T(k)\frac{\begin{bmatrix} x(k) \\ 1 \end{bmatrix}\begin{bmatrix} x(k) \\ 1 \end{bmatrix}^T}{1 + x^T(k)x(k)}\tilde{\rho}(k) = -\frac{\left(\tilde{\rho}^T(k)\begin{bmatrix} x(k) \\ 1 \end{bmatrix}\right)^2}{1 + x^T(k)x(k)}\,. \tag{A29}$$

Define

$$\tau \triangleq \mu(1+\alpha)(\sigma^2+1)b_m^T P b_m\,. \tag{A30}$$

From (22) and (A29) and using (23) in Lemma 2, we have

$$\begin{aligned}
\Delta V(\tilde{x}(k),\tilde{\rho}(k)) &\leq \mu\frac{-\tilde{x}^T(k)R\tilde{x}(k)+\left(\tilde{\rho}^T(k)\begin{bmatrix}x(k)\\1\end{bmatrix}\right)^2(\sigma^2+1)b_m^TPb_m}{1+\mu\tilde{x}^T(k)P\tilde{x}(k)}-\tau\frac{\left(\tilde{\rho}^T(k)\begin{bmatrix}x(k)\\1\end{bmatrix}\right)^2}{1+x^T(k)x(k)}\\
&\leq \mu\frac{-\tilde{x}^T(k)R\tilde{x}(k)+\left(\tilde{\rho}^T(k)\begin{bmatrix}x(k)\\1\end{bmatrix}\right)^2(\sigma^2+1)b_m^TPb_m}{1+\mu\tilde{x}^T(k)P\tilde{x}(k)}-\tau\frac{\left(\tilde{\rho}^T(k)\begin{bmatrix}x(k)\\1\end{bmatrix}\right)^2}{(1+\alpha)(1+\mu\tilde{x}^T(k)P\tilde{x}(k))}\\
&= \mu\frac{-\tilde{x}^T(k)R\tilde{x}(k)+\left(\tilde{\rho}^T(k)\begin{bmatrix}x(k)\\1\end{bmatrix}\right)^2(\sigma^2+1)b_m^TPb_m-\left(\tilde{\rho}^T(k)\begin{bmatrix}x(k)\\1\end{bmatrix}\right)^2(\sigma^2+1)b_m^TPb_m}{1+\mu\tilde{x}^T(k)P\tilde{x}(k)}\\
&= \mu\frac{-\tilde{x}^T(k)R\tilde{x}(k)}{1+\mu\tilde{x}^T(k)P\tilde{x}(k)}\leq 0\,.
\end{aligned} \tag{A31}$$

The above implies that $\tilde{x}(k)$ and $\tilde{\rho}(k)$ are uniformly bounded and that the estimation error dynamics are stable. Then, we have

$$V(\tilde{x}(k'),\tilde{\rho}(k'))\leq\ldots\leq V(\tilde{x}(0),\tilde{\rho}(0))\,. \tag{A32}$$

Since $\tilde{x}(0)=0$, it follows that

$$\begin{aligned}
\ln(1+\mu\tilde{x}^T(k')P\tilde{x}(k'))&\leq V(\tilde{x}(k'),\tilde{\rho}(k'))\\
(1+\mu\tilde{x}^T(k')P\tilde{x}(k'))&\leq e^{V(\tilde{x}(k'),\tilde{\rho}(k'))}\\
\mu\tilde{x}^T(k')P\tilde{x}(k')&\leq e^{V(\tilde{x}(k'),\tilde{\rho}(k'))}-1\,.
\end{aligned} \tag{A33}$$

Finally,

$$\mu\lambda_{\min}(P)\|\tilde{x}(k')\|_\infty^2\leq\mu\tilde{x}^T(k')P\tilde{x}(k')\leq e^{V(\tilde{x}(k'),\tilde{\rho}(k'))}-1\leq e^{V(\tilde{x}(0),\tilde{\rho}(0))}-1\leq e^{\tau\tilde{\rho}^T(0)\tilde{\rho}(0)}-1\,, \tag{A34}$$

and

$$\|\tilde{x}(k')\|_\infty^2\leq\frac{e^{\tau\tilde{\rho}^T(0)\tilde{\rho}(0)}-1}{\mu\lambda_{\min}(P)}\,. \tag{A35}$$

Note that $\rho\in\Theta\times\Xi$ and that the initial parameter estimation error is bounded by $\|\tilde{\rho}(0)\|\leq 2\max_{\rho\in\Theta\times\Xi}\|\rho\|$. Therefore, $\tilde{\rho}^T(0)\tilde{\rho}(0)\leq\rho_{\max}$. Then we can write

$$\|\tilde{x}(k')\|_\infty\leq\sqrt{\frac{e^{\tau\rho_{\max}}-1}{\mu\lambda_{\min}(P)}}=\sqrt{\frac{1}{2}\left(e^{\tau\rho_{\max}}-1\right)\left(1+4nc_1^2\gamma_0^2+4nc_2^2\right)}\,, \tag{A36}$$

where μ is defined in (A20). Notice that the above is equivalent to Assumption 2 with $\frac{1}{2}\left(e^{\tau\rho_{\max}}-1\right)4nc_1^2<1$ as follows:

$$\begin{aligned}
\sqrt{\frac{\frac{1}{2}(e^{\tau\rho_{\max}}-1)\left(1+4nc_2^2\right)}{1-\frac{1}{2}(e^{\tau\rho_{\max}}-1)4nc_1^2}}&\leq\gamma_0\\
\frac{1}{2}\left(e^{\tau\rho_{\max}}-1\right)\left(1+4nc_2^2\right)&\leq\gamma_0^2\left(1-\frac{1}{2}\left(e^{\tau\rho_{\max}}-1\right)4nc_1^2\right)\\
\frac{1}{2}\left(e^{\tau\rho_{\max}}-1\right)\left(1+4nc_1^2\gamma_0^2+4nc_2^2\right)&\leq\gamma_0^2\,.
\end{aligned} \tag{A37}$$

Therefore, (A36) can be rewritten as

$$\|\tilde{x}(k')\|_\infty\leq\gamma_0\,, \tag{A38}$$

which contradicts the inequality in (A21). Hence, the inequality in (24) holds, which concludes the proof. □

A.4 Proof of Lemma 4

The proof of Lemma 4 is found next.

Proof. Recall that the state predictor (16) can be written in the z domain as:

$$\hat{x}(z)=G(z)\hat{\eta}(z)+H(z)C(z)k_g r(z)+\hat{x}_{in}(z) \tag{A39}$$

which leads to the following upper bound for $i \in \mathbb{N} \cup \{0\}$:

$$\|\hat{x}|_i\|_{\ell_\infty} \leq \|G(z)\|_{\ell_1} \|\hat{\eta}|_i\|_{\ell_\infty} + \|k_g H(z) C(z)\|_{\ell_1} \|r|_i\|_{\ell_\infty} + \|\hat{x}_{in}|_i\|_{\ell_\infty} . \tag{A40}$$

Applying the triangular relationship for norms to the bound (24), we have:

$$|\|\hat{x}|_i\|_{\ell_\infty} - \|x|_i\|_{\ell_\infty}| \leq \gamma_0 . \tag{A41}$$

The adaptation law in (4) and (5) ensures that $\hat{\rho}(k) \in \Theta \times \Xi$ and $\|\hat{\eta}|_i\|_{\ell_\infty} \leq L_\theta \|x|_i\|_{\ell_\infty} + L_\xi$. Substituting $\|x|_i\|_{\ell_\infty}$ yields

$$\|\hat{\eta}\|_{\ell_\infty} \leq L_\theta \left(\|\hat{x}|_i\|_{\ell_\infty} + \gamma_0 \right) + L_\xi . \tag{A42}$$

Then, using the bounds on $\|\hat{x}|_i\|_{\ell_\infty}$ in (A40) and $\|\hat{\eta}|_i\|_{\ell_\infty}$ in (A42), and the ℓ_1 norm condition in (9), leads to:

$$\|\hat{x}|_i\|_{\ell_\infty} \leq \frac{\lambda_\theta \gamma_0 + \|G(z)\|_{\ell_1} L_\xi + \|H(z) k_g C(z)\|_{\ell_1} \|r|_i\|_{\ell_\infty} + \|x_{in}|_i\|_{\ell_\infty}}{1 - \lambda_\theta} . \tag{A43}$$

Since the bound on the right hand side is uniform, then $\hat{x}(k)$ is uniformly bounded. □

A.5 Derivation of $H_1(z)$

We first look at a special case of state-to-input stability for linear time-invariant (LTI) systems. Consider an LTI system given by

$$x(z) = (zI - A)^{-1} b u(z) , \tag{A44}$$

where $x(z)$, $u(z)$ are the z-transforms of the system state $x(k)$ and input $u(k)$, $A \in \mathbb{R}^{n \times n}$, $b \in \mathbb{R}^n$, and assume that:

$$G(z) = (zI - A)^{-1} b = \frac{N(z)}{D(z)} , \tag{A45}$$

where $D(z) = \det(zI - A)$ using Cramer's rule, and $N(z)$ is a $n \times 1$ vector with its i^{th} element being a polynomial function

$$N_i(z) = \sum_{j=1}^{n} N_{ij} z^{j-1} . \tag{A46}$$

Lemma 6. If (A, b) is controllable, then the matrix N of entries N_{ij} is full rank.

Proof. Controllability of (A, b) implies that given an initial condition $x(0) = 0$, and arbitrary k_1 and x_{k_1}, there exists $u(\kappa)$, $\kappa \in [0, k_1]$, such that $x(k_1) = x_{k_1}$. If N is not full rank, then there exists a $\psi \in \mathbb{R}^n$, $\psi \neq 0$, such that $\psi^T N(z) = 0$. Thus, for $x(0) = 0$ we have

$$\psi^T x(z) = \psi^T \frac{N(z)}{D(z)} u(z) = 0 , \quad \forall u(z) , \tag{A47}$$

which implies that $x(\kappa) \neq x_{k_1}$ for any κ. The latter contradicts controllability where $x(k_1) = x_{k_1}$ can be an arbitrary point in $\mathbb{R}^n$. As a result, N must be full rank. □

Corollary 1. If the pair (A, b) in (A44) is controllable, then there exists $c_0 \in \mathbb{R}^n$, such that $c_0^T \frac{N(z)}{D(z)}$ has relative degree one, i.e., $\deg(D(z)) - \deg(c_0^T N(z)) = 1$, and $c_0^T N(z)$ has all its zeros in the unit disk.

Proof. It follows from (A45) that for arbitrary vector $c_0 \in \mathbb{R}^n$:

$$c_0^T (zI - A)^{-1} b = \frac{c_0^T N [z^{n-1} \dots 1]^T}{D(z)} , \tag{A48}$$

where $N \in \mathbb{R}^{n \times n}$ is the matrix with its i^{th} row j^{th} column entry N_{ij} introduced in (A46). Since (A, b) is controllable, N is full rank, from Lemma 6. Consider an arbitrary vector $\bar{c} \in \mathbb{R}^n$ such that $\bar{c}[z^{n-1} \dots 1]^T$ is a stable $n-1$ order polynomial, and let $c_0 = (N^{-1})^T \bar{c}$. Then

$$c_0^T (zI - A)^{-1} b = \frac{\bar{c}^T [z^{n-1} \dots 1]^T}{D(z)} \tag{A49}$$

has relative degree 1 with all its zeros in the unit disk. □

Lemma 7. Let the pair (A, b) be controllable and $F(z)$ be an arbitrary strictly-proper BIBO stable transfer function. Then, there exists a proper and stable $G_1(z)$, given by

$$G_1(z) \triangleq \frac{F(z)}{c_0^T G(z)} c_0^T , \tag{A50}$$

where $c_0 \in \mathbb{R}^n$, and $c_0^T G(z)$ is a minimum phase transfer function with relative degree 1, such that

$$F(z)u(z) = G_1(z)x(z)\,. \tag{A51}$$

Proof. From Corollary 1, it follows that there exists $c_0 \in \mathbb{R}^n$ such that $c_0^T G(z)$ has relative degree one, and $c_0^T G(z)$ has all its zeros in the unit disk. Hence,

$$F(z)u(z) = F(z)\frac{c_0^T G(z)}{c_0^T G(z)}u(z) = G_1(z)x(z)\,, \tag{A52}$$

where the properness of $G_1(z)$ is ensured by the fact that $F(z)$ is strictly-proper, while stability follows immediately from its definition. □

Since the pair (A_m, b_m) in (1) is controllable, Lemma 7 implies that

$$H_1(z) \triangleq C(z)\frac{1}{c_0^T H(z)}c_0^T\,, \tag{A53}$$

is proper and BIBO stable.

ACKNOWLEDGEMENTS

The authors would like to thank Naira Hovakimyan and Hamid Jafarnejad for the helpful discussions regarding ℓ_1 adaptive control.

DATA AVAILABILITY STATEMENT

Data sharing not applicable to this article as no datasets were generated or analysed during the current study.

References

1. Skelton R. Model error concepts in control design. *International Journal of Control* 1989; 49(5): 1725–1753.
2. Skogestad S, Postlethwaite I. *Multivariable feedback control: analysis and design*. 2. Wiley New York . 2007.
3. Hovakimyan N, Cao C. $\mathcal{L}_1$ *Adaptive Control Theory: Guaranteed Robustness with Fast Adaptation*. Philadelphia, PA: Society for Industrial and Applied Mathematics . 2010.
4. Michini B, How JP. $\mathcal{L}_1$ Adaptive Control for Indoor Autonomous Vehicles: Design Process and Flight Testing. In: Proc. of the AIAA Guidance, Navigation, and Control Conference. ; 2009: 5754.
5. Jafarnejadsani H, Sun D, Lee H, Hovakimyan N. Optimized $\mathcal{L}_1$ Adaptive Controller for Trajectory Tracking of an Indoor Quadrotor. *Journal of Guidance, Control, and Dynamics* 2017; 40(6): 1415–1427.
6. Maalouf D, Chemori A, Creuze V. L1 adaptive depth and pitch control of an underwater vehicle with real-time experiments. *Ocean Engineering* 2015; 98: 66–77.
7. Harris J, Elliott CM, Tallant GS. Stability and Performance Robustness of an L1 Adaptive Dynamic Inversion Flight Control System. In: AIAA Scitech 2019 Forum. ; 2019: 0141.
8. Nguyen Q, Sreenath K. L1 adaptive control for bipedal robots with control Lyapunov function based quadratic programs. In: Proc. of the American Control Conference (ACC). ; 2015: 862–867.
9. Mallikarjunan S, Nesbit B, Kharisov E, Xargay E, Hovakimyan N, Cao C. $\mathcal{L}_1$ Adaptive Controller for Attitude Control of Multirotors. In: Proc. of the AIAA Guidance, Navigation and Control Conference. ; 2012; Minneapolis, MN.

10. Jafarnejadsani H, Hovakimyan N. Optimal Filter Design for a Discrete-Time Formulation of L1-Adaptive Control. In: AIAA Infotech@ Aerospace. ; 2015: 0119.

11. Jafarnejadsani H, Lee H, Hovakimyan N. An $\mathcal{L}_1$ adaptive control design for output-feedback sampled-data systems. In: Proc. of the American Control Conference (ACC). ; 2017: 5744–5749.

12. Morari M, Lee JH. Model predictive control: past, present and future. *Computers & Chemical Engineering* 1999; 23(4): 667–682.

13. Mayne DQ, Rawlings JB, Rao CV, Scokaert PO. Constrained model predictive control: stability and optimality. *Automatica* 2000; 36(6): 789–814.

14. Camacho EF, Alba CB. *Model predictive control*. Springer Science & Business Media . 2013.

15. Bemporad A, Morari M. Robust model predictive control: A survey. In: Springer. 1999 (pp. 207–226).

16. Rawlings J, Mayne D, Diehl M. *Model Predictive Control: Theory, Computation, and Design*. Nob Hill Publishing, LLC . 2017.

17. Grimm G, Messina MJ, Tuna SE, Teel AR. Examples when nonlinear model predictive control is nonrobust. *Automatica* 2004; 40(10): 1729–1738.

18. Gilbert EG, Kolmanovsky I, Tan KT. Discrete-time reference governors and the nonlinear control of systems with state and control constraints. *International Journal of Robust and Nonlinear Control* 1995; 5(5): 487–504.

19. Lee JH, Yu Z. Worst-case formulations of model predictive control for systems with bounded parameters. *Automatica* 1997; 33(5): 763–781.

20. Kothare MV, Balakrishnan V, Morari M. Robust constrained model predictive control using linear matrix inequalities. *Automatica* 1996; 32(10): 1361–1379.

21. Scokaert PO, Mayne D. Min-max feedback model predictive control for constrained linear systems. *IEEE Transactions on Automatic control* 1998; 43(8): 1136–1142.

22. Mayne DQ, Seron MM, Raković S. Robust model predictive control of constrained linear systems with bounded disturbances. *Automatica* 2005; 41(2): 219–224.

23. Limon D, Alvarado I, Alamo T, Camacho E. Robust tube-based MPC for tracking of constrained linear systems with additive disturbances. *Journal of Process Control* 2010; 20(3): 248–260.

24. Sun Z, Dai L, Liu K, Xia Y, Johansson KH. Robust MPC for tracking constrained unicycle robots with additive disturbances. *Automatica* 2018; 90: 172–184.

25. Goodwin GC, Kong H, Mirzaeva G, Seron MM. Robust model predictive control: reflections and opportunities. *Journal of Control and Decision* 2014; 1(2): 115–148.

26. Fukushima H, Kim TH, Sugie T. Adaptive model predictive control for a class of constrained linear systems based on the comparison model. *Automatica* 2007; 43(2): 301–308.

27. Zhu B, Xia X. Adaptive model predictive control for unconstrained discrete-time linear systems with parametric uncertainties. *IEEE Transactions on Automatic Control* 2015; 61(10): 3171–3176.

28. Tanaskovic M, Fagiano L, Smith R, Morari M. Adaptive receding horizon control for constrained MIMO systems. *Automatica* 2014; 50(12): 3019 - 3029.

29. Lorenzen M, Cannon M, Allgöwer F. Robust MPC with recursive model update. *Automatica* 2019; 103: 461–471.

30. Bujarbaruah M, Zhang X, Tanaskovic M, Borrelli F. Adaptive Stochastic MPC under Time Varying Uncertainty. *IEEE Transactions on Automatic Control* 2020.

31. Adetola V, Guay M. Robust adaptive MPC for constrained uncertain nonlinear systems. *International Journal of Adaptive Control and Signal Processing* 2011; 25(2): 155–167.

32. Piga D, Formentin S, Bemporad A. Direct data-driven control of constrained systems. *IEEE Transactions on Control Systems Technology* 2018; 26(4): 1422–1429.

33. Polverini MP, Formentin S, Merzagora L, Rocco P. Mixed Data-Driven and Model-Based Robot Implicit Force Control: A Hierarchical Approach. *IEEE Transactions on Control Systems Technology* 2020.

34. Lakshmanan A, Gahlawat A, Hovakimyan N. Safe Feedback Motion Planning: A Contraction Theory and $\mathcal{L}_1$-Adaptive Control Based Approach. In: Proc. of the IEEE Conference on Decision and Control (CDC). ; 2020: 1578-1583.

35. Pereida K, Schoellig AP. Adaptive Model Predictive Control for High-Accuracy Trajectory Tracking in Changing Conditions. In: Proc. of the IEEE/RSJ International Conference on Intelligent Robots and Systems (IROS). ; 2018: 7831–7837.

36. Pereida K, Helwa MK, Schoellig AP. Data-efficient multirobot, multitask transfer learning for trajectory tracking. *IEEE Robotics and Automation Letters* 2018; 3(2): 1260–1267.

37. Pereida K, Kooijman D, Duivenvoorden RR, Schoellig AP. Transfer learning for high-precision trajectory tracking through $\mathcal{L}_1$ adaptive feedback and iterative learning. *International Journal of Adaptive Control and Signal Processing* 2019; 33(2): 388–409.

38. Elnaggar M, Saad MS, Fattah HA, Elshafei AL. Discrete time L_1 adaptive control for systems with time-varying parameters and disturbances. In: Proc. of the IEEE Conference on Decision and Control (CDC). ; 2016: 2115–2120.

39. Pereida K, Schoellig AP. Robust Adaptive Model Predictive Control for High-Accuracy Trajectory Tracking in Changing Conditions. In: IEEE International Conference on Robotics and Automation (ICRA) - Workshop on Algorithms and Architectures for Learning in-the-Loop Systems in Autonomous Flight. ; 2019.

40. Goodwin G, Ramadge P, Caines P. Discrete-time multivariable adaptive control. *IEEE Transactions on Automatic Control* 1980; 25(3): 449–456.

41. Goodwin GC, Sin KS. *Adaptive Filtering Prediction and Control*. Prentice Hall . 1984.

42. Akhtar S, Bernstein DS. Lyapunov-stable discrete-time model reference adaptive control. *International Journal of Adaptive Control and Signal Processing* 2005; 19(10): 745–767.

43. Cao C, Hovakimyan N. Design and analysis of a novel l1 adaptive controller, part i: control signal and asymptotic stability. In: Proc. of the American Control Conference (ACC). ; 2006: 3397–3402.

44. Cuzzola FA, Geromel JC, Morari M. An improved approach for constrained robust model predictive control. *Automatica* 2002; 38(7): 1183–1189.

45. Rakovic SV, Kerrigan EC, Kouramas KI, Mayne DQ. Invariant approximations of the minimal robust positively Invariant set. *IEEE Transactions on Automatic Control* 2005; 50(3): 406-410.

46. Kouvaritakis B, Cannon M. *Model Predictive Control: Classical, Robust and Stochastic*. Springer . 2015.

47. Langson W, Chryssochoos I, Raković S, Mayne D. Robust model predictive control using tubes. *Automatica* 2004; 40(1): 125-133.

48. Herceg M, Kvasnica M, Jones C, Morari M. Multi-Parametric Toolbox 3.0. http://control.ee.ethz.ch/~mpt; 2013.

49. Borrelli F, Bemporad A, Morari M. *Predictive Control for Linear and Hybrid Systems*. Cambridge University Press . 2017

50. Andersen MS, Dahl J, Vandenberghe L. CVXOPT: A Python package for convex optimization. cvxopt.org; 2004.